# Adaptive Cooperative Load Transportation by a Team of Quadrotors With Multiple Constraint Requirements

Xu Jin, *Member, IEEE*, and Zhongjun Hu

***Abstract*— Cable-suspended load carried by multiple unmanned aerial vehicles (UAVs) has applications in many areas. However, most existing aerial load transportation works are tailored to a specific type of load transportation tasks, or assume simplified system models or transportation scenarios. Furthermore, no existing works on this topic can provide a unified framework to address multiple performance and safety constraints during the cooperative transportation operation. In this paper, we propose and investigate a new constrained cooperative control architecture for an UAV team, which are collaboratively carrying a three-dimensional load, subject to multiple user-defined time-varying performance and safety constraint requirements. A unified framework using universal barrier functions has been proposed to deal with different types of constraint requirements. Moreover, control saturation and uncertainties in UAV inertia matrices are dealt with by employing adaptive estimators. Exponential convergence on the distance and attitude tracking errors can be guaranteed by the algorithm. Lastly, we discuss a simulation example that further shows the efficacy of the proposed cooperative control framework.**

***Index Terms*— Adaptive cooperative transportation, cable-suspended payload, multiple system constraints.**

## I. Introduction

CABLE-SUSPENDED load transportation by unmanned aerial vehicles (UAVs), especially quadrotors, has attracted significant attention over recent years [1], [2], [3], [4], due to its vertical take-off and landing abilities and wide range of potential applications including search/rescue missions and package delivery. However, a single UAV usually suffers from limited payload capacity, and is prone to failure in the face of mechanical breakdowns. Therefore, it is advantageous to use a group of UAVs to collaboratively transport a common payload together, which is a modular design where the number of UAVs can depend on the mission scenarios.

There has been a fruitful discussion on cooperative aerial load transportation during the past decade. However, most of existing works are tailored to a specific type of aerial load transportation tasks, or assume simplified system models or transportation scenarios. For example, [5], [6] discuss two quadrotors carrying a rod-shaped payload, [7], [8], [9], [10] address quadrotors carrying a dimensionless point-mass payload using three or more multirotor systems, and [11], [12], [13], [14] consider simplified UAV models. These works are not positioned to address a more generic class of load transportation tasks where the load can be a three-dimensional object, and the UAV models are highly nonlinear and uncertain.

To overcome these limitations, other works, including [15], [16], [17], [18], consider more generic operation scenarios, with discussion on more realistic UAV models and/or payload dimensions. Unfortunately, these works only focus on unconstrained system operations during load transportation. In reality, both the UAV team and load need to stay close to the desired path, so that to ensure desirable formation pattern and avoid collision with nearby obstacles. This demands that the cooperative system needs to satisfy certain *performance* constraint requirements. Moreover, for a team of UAVs to cooperatively transport a common load, the distances between any two UAVs in the team cannot be either too small or too large, which can lead to inter-UAV collision and breakdown of the suspension cable, respectively. This implies the load-carrying UAV team needs to satisfy certain *safety* constraint requirements. Failing to address these performance and safety considerations can lead to failures of the cooperative transportation tasks.

To address constrained operations during the load transportation tasks, [19] addresses collision avoidance during path planing, [20] discusses obstacle avoidance for two UAVs when transporting a point-mass payload, [21], [22] consider payload collision avoidance with environment obstacles during transportation, and [23], [24] address constraints in the suspension cable. However, these works fail to discuss constraints for inter-UAV distances during the operation, which is a technically challenging problem due to the interconnections of UAVs via payload. [25] discusses inter-UAV collision avoidance, but ignores constraint requirements on the maximum allowable inter-UAV distances, and fails to consider constraints for the payload movement. Furthermore, most existing works that discuss constrained load transportation tasks, including the aforementioned [22], [23], [24], [25], use optimization-based approaches. Solving the optimization problem in itself puts a high demand for on-board real-time computation, which

Manuscript received 25 April 2022; revised 28 July 2022 and 27 September 2022; accepted 13 October 2022. Date of publication 10 November 2022; date of current version 26 January 2023. This work was supported in part by the National Science Foundation under Grant 2131802. The Associate Editor for this article was L. Wang. *(Corresponding author: Xu Jin.)*

The authors are with the Department of Mechanical and Aerospace Engineering, University of Kentucky, Lexington, KY 40506 USA (e-mail: xu.jin@uky.edu; zhongjunhu@uky.edu).

Digital Object Identifier 10.1109/TITS.2022.3219296

may not be realistic for small-size UAV platforms. Moreover, no existing works, to the best of our knowledge, proposed a unified framework to address both *performance* and *safety* constraint requirements during the cooperative aerial load transportation task, where both the UAV team and the payload need to stay close to the desired trajectories, and the inter-UAV distances cannot be either too small or too large. The main difficulty is due to the coupling of nonlinear dynamics of both the load and the UAVs, which are interconnected via the cables.

In this work, we propose and investigate a new constrained cooperative control architecture for an UAV team, which is collaboratively transporting a cable-suspended three-dimensional rigid-body load. User-defined time-varying performance and safety constraint requirements are considered and addressed under this new and unified formation control architecture. Specifically, to ensure operation performance, constraint requirements on distance tracking errors of the payload and each UAV are addressed. To guarantee safety, we consider safety constraints on the inter-UAV distances, which cannot be either too large or too small. Universal barrier functions [26], [27], [28] are used to deal with the constraint requirements, which can address different types of constraints in a unified framework. Moreover, uncertainties in the UAV inertia matrix, and control saturation effects of UAVs are addressed by the use of adaptive laws. We demonstrate that the proposed cooperative control law can guarantee exponential convergence on the relative distance and attitude tracking errors, with all constraint requirements met during the load transportation operation.

The notations used in this work are fairly standard. Specifically, $\mathbb{R}$ represents the real number set, $\mathbb{R}^+$ represents the non-negative number set, and $I_m$ is the identity matrix in $\mathbb{R}^{m\times m}$. $(\cdot)^{\mathrm{T}}$ denotes the transpose operation, $|\cdot|$ means the absolute value of scalars, and $\|\cdot\|$ represents vectors' Euclidean norm or matrices' induced norm. Furthermore, we use $\mathrm{c}\theta$ to denote $\cos\theta$, $\mathrm{s}\theta$ to denote $\sin\theta$, and $\mathrm{t}\theta$ to denote $\tan\theta$. We also write $\dot{(\cdot)}$ as the first order time derivative of $(\cdot)$, if $(\cdot)$ is differentiable. Next, $\mathrm{C}^n$ denotes the class of functions that are $n$-times differentiable with respect to time, with the derivatives being in the class of $\mathrm{C}^{n-1}$. Besides, for any two vectors $v_1,\ v_2 \in \mathbb{R}^3$, the cross-product operator $\mathbb{S}(\cdot)$ gives $\mathbb{S}(v_1)v_2 = v_1 \times v_2$. It is also true that $\mathbb{S}(v_1)v_2 = -\mathbb{S}(v_2)v_1$ and $v_1^{\mathrm{T}}\mathbb{S}(v_2)v_1 = 0$. Finally, $\mathrm{SO}(3) = \{\Omega \in \mathbb{R}^{3\times3} \mid \Omega^{\mathrm{T}}\Omega = I_3\}$ is a set of orthogonal matrices in $\mathbb{R}^{3\times3}$, and $\mathrm{S}^2 = \{x \in \mathbb{R}^3 \mid \|x\| = 1\}$ is a set of unit vectors in $\mathbb{R}^3$.

## II. Problem Formulation

### A. System Dynamics

Consider a group of $N$ ($N \geq 3$) UAVs that are cooperatively transporting a rigid body payload connected via cables (for example, see Figure 1), where the dynamics are given as

$$\text{UAVs}\begin{cases} m_i\ddot{p}_i(t) = -\mathrm{sat}\big(F_i(t)\big)R(\Theta_i(t))e_z + m_i g e_z \\ \qquad\qquad +T_i(t)R(\Theta_{\mathrm{L}}(t))e_i(t) \\ \dot{\Theta}_i(t) = \Gamma(\Theta_i(t))\omega_i(t) \\ J_i\dot{\omega}_i(t) + \mathbb{S}(\omega_i(t))J_i\omega_i(t) = \tau_i(t), \end{cases} \tag{1}$$

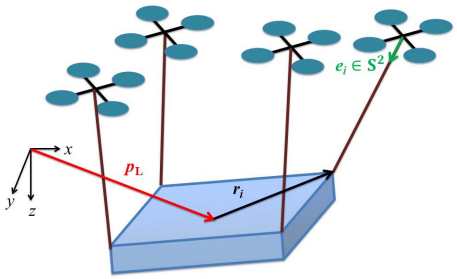


Fig. 1. Cable-suspended load transportation by UAVs (illustration only).

$$\text{Load}\begin{cases} m_{\mathrm{L}}\ddot{p}_{\mathrm{L}}(t) = m_{\mathrm{L}} g e_z - \sum_{i=1}^{N} T_i(t)R(\Theta_{\mathrm{L}}(t))e_i(t) \\ \dot{\Theta}_{\mathrm{L}}(t) = \Gamma(\Theta_{\mathrm{L}}(t))\omega_{\mathrm{L}}(t) \\ J_{\mathrm{L}}\dot{\omega}_{\mathrm{L}}(t) + \mathbb{S}(\omega_{\mathrm{L}}(t))J_{\mathrm{L}}\omega_{\mathrm{L}}(t) \\ \qquad\qquad = \sum_{i=1}^{N} \mathbb{S}(r_i)(-T_i(t)e_i(t)), \end{cases} \tag{2}$$

where $m_i \in \mathbb{R}^+$ is the mass of the $i$th quadrotor ($i = 1, \cdots, N$), and $J_i \in \mathbb{R}^{3\times3}$ is a symmetric positive definite matrix representing the inertia. The position and attitude in the inertial reference frame are represented as $p_i(t) = [x_i(t),\ y_i(t),\ z_i(t)]^{\mathrm{T}} \in \mathbb{R}^3$ and $\Theta_i(t) = [\phi_i(t),\ \theta_i(t),\ \psi_i(t)]^{\mathrm{T}} \in \mathbb{R}^3$, respectively. $R(\Theta_i(t)) \in \mathrm{SO}(3)$ is the rotation matrix, which relates the body-fixed frame to the inertial frame and is expressed as

$$R(\Theta_i) = \begin{bmatrix} \mathrm{c}\theta_i\mathrm{c}\psi_i & \mathrm{s}\phi_i\mathrm{s}\theta_i\mathrm{c}\psi_i - \mathrm{c}\phi_i\mathrm{s}\psi_i & \mathrm{c}\phi_i\mathrm{s}\theta_i\mathrm{c}\psi_i + \mathrm{s}\phi_i\mathrm{s}\psi_i \\ \mathrm{c}\theta_i\mathrm{s}\psi_i & \mathrm{s}\phi_i\mathrm{s}\theta_i\mathrm{s}\psi_i + \mathrm{c}\phi_i\mathrm{c}\psi_i & \mathrm{c}\phi_i\mathrm{s}\theta_i\mathrm{s}\psi_i - \mathrm{s}\phi_i\mathrm{c}\psi_i \\ -\mathrm{s}\theta_i & \mathrm{s}\phi_i\mathrm{c}\theta_i & \mathrm{c}\phi_i\mathrm{c}\theta_i \end{bmatrix}. \tag{3}$$

The rotational velocities with respect to this body-fixed frame are denoted by $\omega_i(t) = [\omega_{xi}(t),\ \omega_{yi}(t),\ \omega_{zi}(t)]^{\mathrm{T}} \in \mathbb{R}^3$, and $\Gamma(\Theta_i(t))$ is the transformation matrix that relates the angular velocity in the body-fixed frame to the rate of change of the Euler angles in the inertial frame, and is given by

$$\Gamma(\Theta_i) = \begin{bmatrix} 1 & \mathrm{s}\phi_i\mathrm{t}\theta_i & \mathrm{c}\phi_i\mathrm{t}\theta_i \\ 0 & \mathrm{c}\phi_i & -\mathrm{s}\phi_i \\ 0 & \mathrm{s}\phi_i/\mathrm{c}\theta_i & \mathrm{c}\phi_i/\mathrm{c}\theta_i \end{bmatrix}, \tag{4}$$

which is well defined and invertable when $-\frac{\pi}{2} < \phi_i(t) < \frac{\pi}{2}$ and $-\frac{\pi}{2} < \theta_i(t) < \frac{\pi}{2}$. Furthermore, $g \in \mathbb{R}$ is the gravitational acceleration and $e_z = [0,\ 0,\ 1]^{\mathrm{T}} \in \mathbb{R}^3$ is the unit vector. Next, $T_i(t) \in \mathbb{R}^+$ represents the tension in the $i$th rigid cable, $\mathrm{sat}\big(F_i(t)\big) \in \mathbb{R}^+$ denotes the thrust of the $i$th quadrotor $F_i(t) \in \mathbb{R}^+$ ($i = 1, \cdots, N$) which is subject to saturation nonlinearity described in [29]:

$$\mathrm{sat}\big(F_i(t)\big) = \begin{cases} F_{Mi}, & F_i(t) \geq F_{Mi} \\ F_i(t), & F_i(t) < F_{Mi} \end{cases},$$

where $F_{Mi}$ is the saturation limit for thrust $F_i(t)$ and $\mathrm{sign}(\cdot)$ is the sign function. Finally, $\tau_i(t) \in \mathbb{R}^3$ represents the torques of the $i$th quadrotor ($i = 1, \cdots, N$).

Similarly, $m_{\rm L} \in \mathbb{R}^+$ is the load mass, and $J_{\rm L} \in \mathbb{R}^{3\times3}$ is the load inertia that is symmetric and positive definite, where the subscript L stands for "Load". $p_{\rm L}(t) = [x_{\rm L}(t),\ y_{\rm L}(t),\ z_{\rm L}(t)]^{\rm T} \in \mathbb{R}^3$ and $\Theta_{\rm L}(t) = [\phi_{\rm L}(t),\ \theta_{\rm L}(t),\ \psi_{\rm L}(t)]^{\rm T} \in \mathbb{R}^3$ represent the load position and attitude in the inertial reference frame, respectively, and $\omega_{\rm L}(t) = [\omega_{x{\rm L}}(t),\ \omega_{y{\rm L}}(t),\ \omega_{z{\rm L}}(t)]^{\rm T} \in \mathbb{R}^3$ represents the load rotational velocity with respect to its body-fixed frame. Furthermore, as shown in Figure 1, $r_i \in \mathbb{R}^3$ is the attachment point on the payload by the $i$th link, represented in the payload body-fixed frame. Finally, $e_i(t) \in {\rm S}^2$ is the unit direction vector from the $i$th UAV mass center towards the $i$th link attachment point.

As shown in Appendix A (see (66)–(74)), the angular motion dynamics of the UAV can be rewritten as

$$M_i(\Theta_i(t))\ddot{\Theta}_i(t) + C_i(\Theta_i(t), \dot{\Theta}_i(t))\dot{\Theta}_i(t) = \Psi^{\rm T}(\Theta_i(t))J_i^{\rm T}\tau_i(t), \tag{5}$$

where $\Psi(\Theta_i(t))$, $M_i(\Theta_i(t))$, and $C_i(\Theta_i(t), \dot{\Theta}_i(t))$ are given in (66), (70), and (71), respectively. Similarly

$$M_{\rm L}(\Theta_{\rm L}(t))\ddot{\Theta}_{\rm L}(t) + C_{\rm L}(\Theta_{\rm L}(t), \dot{\Theta}_{\rm L}(t))\dot{\Theta}_{\rm L}(t) = \Psi^{\rm T}(\Theta_{\rm L}(t))J_{\rm L}^{\rm T}\sum_{i=1}^{N}\mathbb{S}(r_i)(-T_i(t)e_i(t)), \tag{6}$$

where $M_{\rm L}(\Theta_{\rm L}(t))$, and $C_{\rm L}(\Theta_{\rm L}(t), \dot{\Theta}_{\rm L}(t))$ are given in (73) and (74), respectively.

### B. System Constraint Requirements

In the cooperative transportation task, the payload is supposed to track its desired trajectory, denoted by $p_{\rm dL}(t) \triangleq [x_{\rm dL}(t),\ y_{\rm dL}(t),\ z_{\rm dL}(t)]^{\rm T} \in \mathbb{R}^3$. Moreover, all UAVs need to track a desired formation pattern, with the coordinate of the reference trajectory for the $i$th vehicle ($i = 1, \cdots, N$) denoted by $p_{{\rm d}i}(t) \triangleq [x_{{\rm d}i}(t),\ y_{{\rm d}i}(t),\ z_{{\rm d}i}(t)]^{\rm T} \in \mathbb{R}^3$.

Now, define the line-of-sight (LOS) distance tracking error for the payload $d_{\rm eL}(t)$ as

$$d_{\rm eL} \triangleq \sqrt{(x_{\rm L} - x_{\rm dL})^2 + (y_{\rm L} - y_{\rm dL})^2 + (z_{\rm L} - z_{\rm dL})^2}, \tag{7}$$

which is the distance between the desired and actual position of the payload. Furthermore, for the $i$th quadrotor ($i = 1, \cdots, N$), define the line-of-sight distance tracking error $d_{{\rm e}i}(t)$ as

$$d_{{\rm e}i} \triangleq \sqrt{(x_i - x_{{\rm d}i})^2 + (y_i - y_{{\rm d}i})^2 + (z_i - z_{{\rm d}i})^2}. \tag{8}$$

Besides, the desired LOS relative distance between any two quadrotors $\vartheta_{ij}(t)$ is formulated as

$$\vartheta_{ij} \triangleq \sqrt{(x_{{\rm d}i} - x_{{\rm d}j})^2 + (y_{{\rm d}i} - y_{{\rm d}j})^2 + (z_{{\rm d}i} - z_{{\rm d}j})^2}, \tag{9}$$

and the actual LOS relative distance $d_{ij}(t)$ is

$$d_{ij} \triangleq \sqrt{(x_i - x_j)^2 + (y_i - y_j)^2 + (z_i - z_j)^2}. \tag{10}$$

The configurations in the case of three quadrotors can be seen in Figure 2.

During the cooperative transportation, there are certain **system constraint requirements** that need to be satisfied,

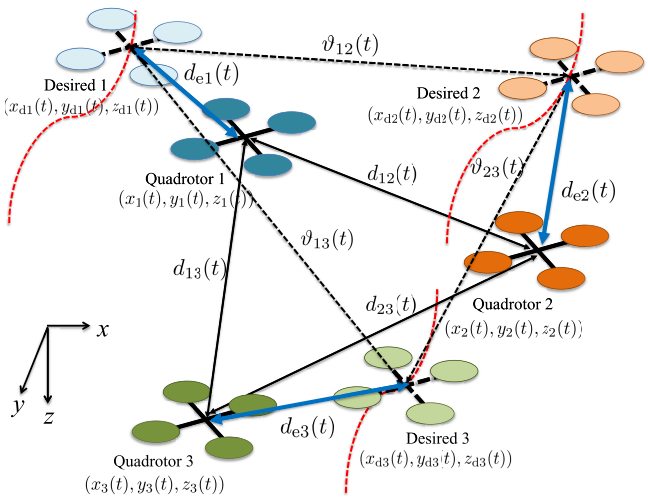


Fig. 2. Illustration in the case of three quadrotors: for $i, j = 1, 2, 3$, $j \neq i$, quadrotors represented in dark colors and solid black are the real-time positions ($x_i(t)$, $y_i(t)$, $z_i(t)$), quadrotors represented in light colors and dashed black are the reference locations ($x_{{\rm d}i}(t)$, $y_{{\rm d}i}(t)$, $z_{{\rm d}i}(t)$), dashed lines in red are the desired path for each UAV, dashed lines in black are the desired inter-quadrotor distances $\vartheta_{ij}(t)$, solid lines in black are the real-time inter-quadrotor distances $d_{ij}(t)$, and solid lines in blue are the real-time distance tracking errors $d_{{\rm e}i}(t)$.

in order to ensure the *precise* and *safe* functioning of the system. First, the payload position tracking error $d_{\rm eL}(t)$ needs to meet the *performance constraint* requirement that

$$d_{\rm eL}(t) < \Omega_{d{\rm HL}}(t), \tag{11}$$

where, for all $t \geq 0$, $\Omega_{d{\rm HL}}(t) > 0$ is a time-varying constraint function that can be user defined, and is $C^3$. This means the payload should not deviate much from its desired trajectory. Moreover, $d_{{\rm e}i}(t)$ has to meet the user-defined *performance constraint*

$$d_{{\rm e}i}(t) < \Omega_{d{\rm H}i}(t), \tag{12}$$

where $\Omega_{d{\rm H}i}(t) > 0$ is a time-varying constraint function, and is $C^3$. This means each UAV cannot deviate too much from its desired trajectory.

Next, define the LOS relative distance tracking error between the $i$th and $j$th quadrotors ($i, j = 1, \cdots, N$, $j \neq i$) as $d_{{\rm e}ij}(t) \triangleq d_{ij}(t) - \vartheta_{ij}(t)$, which has to meet the following *safety constraint*

$$-\Omega_{{\rm W}ij}(t) < d_{{\rm e}ij}(t) < \Omega_{{\rm H}ij}(t), \tag{13}$$

where $\Omega_{{\rm H}ij}(t) > 0$ is the upper constraint for $d_{{\rm e}ij}(t)$, and $-\Omega_{{\rm W}ij}(t) < 0$ is the lower bound, with $0 < \Omega_{{\rm W}ij}(t) < \vartheta_{ij}(t)$. Both $\Omega_{{\rm H}ij}(t)$ and $\Omega_{{\rm W}ij}(t)$ are $C^3$. The constraint requirement (13) means that the inter-quadrotor distance cannot be either too large or too small.

*Remark 1:* Both (11) and (12) belong to the *performance* constraint requirements. The physical meaning is that during the cooperative load transportation, both the load and the UAV team should stay close to the desired trajectories. Violation of such performance constraint requirements will result in failure to keep the desired formation and/or collisions with environment boundaries. (13) belongs to the *safety* constraint

requirement. The physical meaning is that any two UAVs in the team cannot be too close or too far apart, which will result in inter-UAV collisions or the suspension cables being over stretched, respectively.

### C. Control Objective

The **control objective** for the cooperative transportation problem is to design a control framework such that:

1) The payload distance tracking error $d_{\mathrm{eL}}(t)$ and the UAV distance tracking errors $d_{ei}(t)$ $(i = 1, \cdots, N)$ can all converge into arbitrarily small neighbourhoods of zero;

2) The relative distance errors $d_{eij}(t)$ between any two quadrotors can converge into arbitrarily small neighbourhoods of zero;

3) The payload attitude tracking error $\Theta_{\mathrm{L}}(t) - \Theta_{\mathrm{dL}}(t)$ and the UAV attitude tracking errors $\Theta_i(t) - \Theta_{\mathrm{d}i}(t)$ can converge into arbitrarily small neighbourhoods of zero;

4) The system constraint requirements (11), (12), and (13) are met during the operation.

We now present the following assumptions that will be used in the theoretical analysis and controller synthesis.

*Assumption 1:* The payload reference trajectory $x_{\mathrm{dL}}(t)$, $y_{\mathrm{dL}}(t)$, and $z_{\mathrm{dL}}(t)$ are all $\mathrm{C}^3$, and for the $i$th quadrotor $(i = 1, \cdots, N)$ $x_{\mathrm{d}i}(t)$, $y_{\mathrm{d}i}(t)$, and $z_{\mathrm{d}i}(t)$ are $\mathrm{C}^3$. Moreover, the reference payload attitude $\Theta_{\mathrm{dL}}(t)$ is $\mathrm{C}^3$, and the reference yaw angle $\psi_{\mathrm{d}i}(t)$ is $\mathrm{C}^2$.

*Assumption 2:* The cables are massless and cannot be stretched, and the tensions in the cables are *unknown* but bounded.

*Assumption 3:* The payload mass $m_{\mathrm{L}}$ and UAV mass $m_i$ for the $i$th quadrotor $(i = 1, \cdots, N)$ are known. However, the payload inertia $J_{\mathrm{L}}$ and UAV inertia $J_i$ are *unknown*, and are assumed to be both upper and lower bounded, such that for any $z \in \mathbb{R}^3$, $\underline{J}_{\mathrm{L}} z^{\mathrm{T}} z < z^{\mathrm{T}} J_{\mathrm{L}} z < \bar{J}_{\mathrm{L}} z^{\mathrm{T}} z$ and $\underline{J}_i z^{\mathrm{T}} z < z^{\mathrm{T}} J_i z < \bar{J}_i z^{\mathrm{T}} z$, where $\bar{J}_{\mathrm{L}}$, $\underline{J}_{\mathrm{L}}$, $\bar{J}_i$, and $\underline{J}_i$ are *unknown* positive constants. As a direct result, the symmetric positive definite matrices $M_i(\Theta_i)$ and $M_{\mathrm{L}}(\Theta_{\mathrm{L}})$ in (70) and (73), respectively, are both *unknown* and bounded, such that for any $z \in \mathbb{R}^3$, $\underline{M}_i z^{\mathrm{T}} z < z^{\mathrm{T}} M_i(\Theta_i) z < \bar{M}_i z^{\mathrm{T}} z$ and $\underline{M}_{\mathrm{L}} z^{\mathrm{T}} z < z^{\mathrm{T}} M_{\mathrm{L}}(\Theta_{\mathrm{L}}) z < \bar{M}_{\mathrm{L}} z^{\mathrm{T}} z$, where $\bar{M}_i$, $\underline{M}_i$, $\bar{M}_{\mathrm{L}}$, and $\underline{M}_{\mathrm{L}}$ are *unknown* constants.

*Assumption 4 ([16]):* Let

$$P = \begin{bmatrix} I_3 & I_3 & \cdots & I_3 \\ \mathbb{S}(r_1) & \mathbb{S}(r_2) & \cdots & \mathbb{S}(r_N) \end{bmatrix} \in \mathbb{R}^{6\times 3N}, \tag{14}$$

we assume $\mathrm{rank}(P) = 6$.

*Remark 2:* This full row rank assumption in Assumption 4 can be realized when $N \geq 3$.

*Assumption 5:* The UAV and load attitudes satisfy $-\frac{\pi}{2} < \phi_{\mathrm{L}}(t) < \frac{\pi}{2}$, $-\frac{\pi}{2} < \theta_{\mathrm{L}}(t) < \frac{\pi}{2}$, $-\frac{\pi}{2} < \phi_i(t) < \frac{\pi}{2}$, and $-\frac{\pi}{2} < \theta_i(t) < \frac{\pi}{2}$, where $i = 1, \cdots, N$.

*Remark 3:* Assumption 5 is necessary to ensure that $\Gamma(\Theta_i(t))$ defined in (4), as well as $\Gamma(\Theta_{\mathrm{L}}(t))$, are both invertable.

In order to simplify representations of signals, we will omit the time and state dependence of signals for the rest of the discussion in this work.

## III. Universal Barrier Function (UBF)

Here we introduce the UBF to be used later in the analysis, which is modified from our earlier work [26] to address the issue of constraint requirements that can be time-varying and asymmetric. Specifically, to address the constraint requirements (11), (12), and (13), the following transformed error variables are introduced for the load and quadrotors as follows

$$\eta_{\mathrm{eL}} = \frac{\Omega_{d\mathrm{HL}} d_{\mathrm{eL}}}{\Omega_{d\mathrm{HL}} - d_{\mathrm{eL}}}, \quad \eta_{ei} = \frac{\Omega_{d\mathrm{H}i} d_{ei}}{\Omega_{d\mathrm{H}i} - d_{ei}},$$
$$\eta_{eij} = \frac{\Omega_{\mathrm{H}ij}\Omega_{\mathrm{W}ij} d_{eij}}{(\Omega_{\mathrm{H}ij} - d_{eij})(\Omega_{\mathrm{W}ij} + d_{eij})}. \tag{15}$$

The universal barrier functions used to deal with the constraint requirements (11), (12), and (13) for the $i$th quadrotor $(i = 1, \cdots, N)$ are then defined as

$$V_{\mathrm{eL}} = \frac{1}{2}\eta_{\mathrm{eL}}^2, \quad V_{ei} = \frac{1}{2}\eta_{ei}^2, \quad V_{eij} = \frac{1}{2}\eta_{eij}^2. \tag{16}$$

Take $V_{eij}$ for an example. It is easy to see that $\eta_{eij} = 0$ if and only if $d_{eij} = 0$. Besides, when $d_{eij} \to \Omega_{\mathrm{H}ij}$, we have $\eta_{eij} \to +\infty$, hence $V_{eij} \to +\infty$. Alternatively, when $d_{eij} \to -\Omega_{\mathrm{W}ij}$, we have $\eta_{eij} \to -\infty$, therefore $V_{eij} \to +\infty$.

## IV. Control Synthesis and Analysis

In this section we present the backstepping controller synthesis procedure, followed by our main theoretical results. The main idea is to first treat the cables as "actuators" for the payload, and design the "desired cable tension" for the payload to track the desired payload trajectory. Then design the UAV control laws with the "desired cable tension" to achieve the desired formation pattern tracking.

The next lemma will be used in the controller synthesis.

*Lemma 1:* For any $\varepsilon > 0$ and any $z \in \mathbb{R}$, we have $0 \leq |z| - \frac{z^2}{\sqrt{z^2+\varepsilon^2}} < \varepsilon$.

### A. "Desired Cable Tension" Design

*Step 1:*

We first consider the position kinematics of the payload. The time derivative of the UBF $V_{\mathrm{eL}}$ leads to

$$\begin{aligned}\dot{V}_{\mathrm{eL}} &= \eta_{\mathrm{eL}}\dot{\eta}_{\mathrm{eL}} = \eta_{\mathrm{eL}}\left[\frac{\partial \eta_{\mathrm{eL}}}{\partial \Omega_{\mathrm{dHL}}}\dot{\Omega}_{\mathrm{dHL}} + \frac{\partial \eta_{\mathrm{eL}}}{\partial d_{\mathrm{eL}}}\dot{d}_{\mathrm{eL}}\right] \\ &= \eta_{\mathrm{eL}}\left[\frac{\partial \eta_{\mathrm{eL}}}{\partial \Omega_{\mathrm{dHL}}}\dot{\Omega}_{\mathrm{dHL}} + \frac{\partial \eta_{\mathrm{eL}}}{\partial d_{\mathrm{eL}}}\frac{1}{d_{\mathrm{eL}}}\Big((x_{\mathrm{L}} - x_{\mathrm{dL}})\dot{x}_{\mathrm{L}}\right. \\ &\quad \left. + (y_{\mathrm{L}} - y_{\mathrm{dL}})\dot{y}_{\mathrm{L}} + (z_{\mathrm{L}} - z_{\mathrm{dL}})\dot{z}_{\mathrm{L}} - \xi_{\mathrm{L}}\Big)\right],\end{aligned} \tag{17}$$

where

$$\xi_{\mathrm{L}} = (x_{\mathrm{L}} - x_{\mathrm{dL}})\dot{x}_{\mathrm{dL}} + (y_{\mathrm{L}} - y_{\mathrm{dL}})\dot{y}_{\mathrm{dL}} + (z_{\mathrm{L}} - z_{\mathrm{dL}})\dot{z}_{\mathrm{dL}}.$$

Now, denote $E_{\mathrm{L}} = \frac{1}{d_{\mathrm{eL}}}[x_{\mathrm{L}} - x_{\mathrm{dL}},\ y_{\mathrm{L}} - y_{\mathrm{dL}},\ z_{\mathrm{L}} - z_{\mathrm{dL}}]^{\mathrm{T}} \in \mathbb{R}^3$, note that $E_{\mathrm{L}}^{\mathrm{T}} E_{\mathrm{L}} = 1$. Furthermore, let $z_{2\mathrm{L}} = \dot{p}_{\mathrm{L}} - \alpha_{p\mathrm{L}}$, we design the stabilizing function $\alpha_{p\mathrm{L}}$ as

$$\alpha_{p\mathrm{L}} = \frac{E_{\mathrm{L}}}{\frac{\partial \eta_{\mathrm{eL}}}{\partial d_{\mathrm{eL}}}}\Big(-\frac{\partial \eta_{\mathrm{eL}}}{\partial \Omega_{\mathrm{dHL}}}\dot{\Omega}_{\mathrm{dHL}} - K_{1\mathrm{L}}\eta_{\mathrm{eL}}\Big) + \dot{p}_{\mathrm{dL}}, \tag{18}$$

where $\frac{\partial \eta_{\mathrm{eL}}}{\partial d_{\mathrm{eL}}} = \frac{\Omega_{d\mathrm{HL}}^2}{(\Omega_{d\mathrm{HL}} - d_{\mathrm{eL}})^2} > 0$, and $K_{1\mathrm{L}} > 0$ is a control constant. Therefore, (17) further leads to

$$\dot{V}_{\mathrm{eL}} = \eta_{\mathrm{eL}} \frac{\partial \eta_{\mathrm{eL}}}{\partial d_{\mathrm{eL}}} E_{\mathrm{L}}^{\mathrm{T}} z_{2\mathrm{L}} - K_{1\mathrm{L}} \eta_{\mathrm{eL}}^2. \tag{19}$$

*Step 2:*

Now we address the translational dynamics of the payload. Design the Lyapunov function candidate as $V_{2\mathrm{L}} = \frac{1}{2} m_{\mathrm{L}} z_{2\mathrm{L}}^{\mathrm{T}} z_{2\mathrm{L}}$, and its time derivative leads to

$$\begin{aligned}\dot{V}_{2\mathrm{L}} &= z_{2\mathrm{L}}^{\mathrm{T}} \Big[ m_{\mathrm{L}} \ddot{p}_{\mathrm{L}} - m_{\mathrm{L}} \dot{\alpha}_{p\mathrm{L}} \Big] \\ &= z_{2\mathrm{L}}^{\mathrm{T}} \Big[ - \sum_{i=1}^{N} T_{\mathrm{d}i} R_{\mathrm{dL}} e_{\mathrm{d}i} - \sum_{i=1}^{N} T_{\mathrm{d}i} (R_{\mathrm{L}} - R_{\mathrm{dL}}) e_{\mathrm{d}i} \\ &\quad + \sum_{i=1}^{N} R_{\mathrm{L}} (T_{\mathrm{d}i} e_{\mathrm{d}i} - T_i e_i) + m_{\mathrm{L}} g e_z - m_{\mathrm{L}} \dot{\alpha}_{p\mathrm{L}} \Big], \end{aligned} \tag{20}$$

where $R_{\mathrm{L}} \triangleq R(\Theta_{\mathrm{L}}(t))$, $R_{\mathrm{dL}} \triangleq R(\Theta_{\mathrm{dL}}(t))$, and $T_{\mathrm{d}i} \triangleq T_{\mathrm{d}i}(t)$ is the desired cable tension in the $i$th cable. Under Assumption 3 and Lemma 1, we have

$$\begin{aligned} & z_{2\mathrm{L}}^{\mathrm{T}} \Big[ - \sum_{i=1}^{N} T_{\mathrm{d}i} (R_{\mathrm{L}} - R_{\mathrm{dL}}) e_{\mathrm{d}i} + \sum_{i=1}^{N} R_{\mathrm{L}} (T_{\mathrm{d}i} e_{\mathrm{d}i} - T_i e_i) \Big] \\ & \quad \le \|z_{2\mathrm{L}}\| \bar{\delta}_{1\mathrm{L}} < \varepsilon_{\mathrm{L}} \bar{\delta}_{1\mathrm{L}} + \bar{\delta}_{1\mathrm{L}} \frac{\|z_{2\mathrm{L}}\|^2}{\sqrt{\|z_{2\mathrm{L}}\|^2 + \varepsilon_{\mathrm{L}}^2}}, \end{aligned}$$

with $\bar{\delta}_{1\mathrm{L}} > 0$ being an *unknown* upper bound, and $\varepsilon_{\mathrm{L}}$ being a small positive constant.

Next, treat $-\sum_{i=1}^{N} T_{\mathrm{d}i} R_{\mathrm{dL}} e_{\mathrm{d}i}$ in (20) as a virtual control signal, represent it as $-F_{\mathrm{dL}}$ for convenience, and design it as

$$\begin{aligned} & - \sum_{i=1}^{N} T_{\mathrm{d}i} R_{\mathrm{dL}} e_{\mathrm{d}i} \\ &= -F_{\mathrm{dL}} \\ &= -m_{\mathrm{L}} g e_z + m_{\mathrm{L}} \dot{\alpha}_{p\mathrm{L}} - K_{2\mathrm{L}} z_{2\mathrm{L}} - \eta_{\mathrm{eL}} \frac{\partial \eta_{\mathrm{eL}}}{\partial d_{\mathrm{eL}}} E_{\mathrm{L}} \\ &\quad - \hat{\delta}_{1\mathrm{L}} \frac{z_{2\mathrm{L}}}{\sqrt{\|z_{2\mathrm{L}}\|^2 + \varepsilon_{\mathrm{L}}^2}}, \end{aligned} \tag{21}$$

where $K_{2\mathrm{L}} > 0$ is a control constant, and $\hat{\delta}_{1\mathrm{L}}$ is the adaptive estimate of the *unknown* constant $\bar{\delta}_{1\mathrm{L}}$, which is designed as

$$\dot{\hat{\delta}}_{1\mathrm{L}} = n_{\delta 1\mathrm{L}} \frac{\|z_{2\mathrm{L}}\|^2}{\sqrt{\|z_{2\mathrm{L}}\|^2 + \varepsilon_{\mathrm{L}}^2}} - \sigma_{\delta 1\mathrm{L}} \hat{\delta}_{1\mathrm{L}}, \tag{22}$$

with $n_{\delta 1\mathrm{L}}$ and $\sigma_{\delta 1\mathrm{L}}$ being positive adaptive gains.

Now, design the Lyapunov function as

$$V_{\mathrm{Load1}} = V_{\mathrm{eL}} + V_{2\mathrm{L}} + V_{\delta 1\mathrm{L}}, \quad V_{\delta 1\mathrm{L}} = \frac{1}{2 n_{\delta 1\mathrm{L}}} \tilde{\delta}_{1\mathrm{L}}^2, \tag{23}$$

where $\tilde{\delta}_{1\mathrm{L}} = \hat{\delta}_{1\mathrm{L}} - \bar{\delta}_{1\mathrm{L}}$, and from (19), (20), (21), and (22), we can get

$$\dot{V}_{\mathrm{Load1}} < -K_{1\mathrm{L}} \eta_{\mathrm{eL}}^2 - K_{2\mathrm{L}} z_{2\mathrm{L}}^{\mathrm{T}} z_{2\mathrm{L}} - \frac{\sigma_{\delta 1\mathrm{L}}}{2 n_{\delta 1\mathrm{L}}} \tilde{\delta}_{1\mathrm{L}}^2 + c_{1\mathrm{L}}, \tag{24}$$

where $c_{1\mathrm{L}} \triangleq \Big( \varepsilon_{\mathrm{L}} \bar{\delta}_{1\mathrm{L}} + \frac{\sigma_{\delta 1\mathrm{L}}}{2 n_{\delta 1\mathrm{L}}} \bar{\delta}_{1\mathrm{L}}^2 \Big)$ is a constant.

*Step 3:*

Next, we discuss the attitude kinematics of the payload. Define $z_{3\mathrm{L}} = \Theta_{\mathrm{L}} - \Theta_{\mathrm{dL}}$ and $z_{4\mathrm{L}} = \dot{\Theta}_{\mathrm{L}} - \alpha_{\Theta\mathrm{L}}$, where the stabilizing function is designed as

$$\alpha_{\Theta\mathrm{L}} = -K_{3\mathrm{L}} z_{3\mathrm{L}} + \dot{\Theta}_{\mathrm{dL}}, \tag{25}$$

where $K_{3\mathrm{L}} > 0$ is a control constant. Now, design the Lyapunov function candidate as $V_{3\mathrm{L}} = \frac{1}{2} z_{3\mathrm{L}}^{\mathrm{T}} z_{3\mathrm{L}}$, its derivative gives rise to

$$\dot{V}_{3\mathrm{L}} = -K_{3\mathrm{L}} z_{3\mathrm{L}}^{\mathrm{T}} z_{3\mathrm{L}} + z_{3\mathrm{L}}^{\mathrm{T}} z_{4\mathrm{L}}. \tag{26}$$

*Step 4:*

Finally, for the load dynamics control, we design the Lyapunov function candidate as $V_{4\mathrm{L}} = \frac{1}{2} z_{4\mathrm{L}}^{\mathrm{T}} M_{\mathrm{L}} z_{4\mathrm{L}}$. With some algebraic analysis shown in Appendix B (see (75)–(77)), treat $\sum_{i=1}^{N} \mathbb{S}(r_i)(-T_{\mathrm{d}i} e_{\mathrm{d}i})$ in (75) as a virtual control signal, represent it as $-M_{\mathrm{dL}}$ for convenience, and design it as

$$\begin{aligned} \sum_{i=1}^{N} \mathbb{S}(r_i)(-T_{\mathrm{d}i} e_{\mathrm{d}i}) &= -M_{\mathrm{dL}} \\ &= -\frac{\Psi_{\mathrm{L}} z_{4\mathrm{L}} \|\bar{\mu}_{\mathrm{L}}\|^2 \hat{\rho}_{J\mathrm{L}}^2}{\sqrt{\|\Psi_{\mathrm{L}} z_{4\mathrm{L}}\|^2 \|\bar{\mu}_{\mathrm{L}}\|^2 \hat{\rho}_{J\mathrm{L}}^2 + \varepsilon_{\mathrm{L}}^2}}, \end{aligned} \tag{27}$$

where

$$\begin{aligned} \bar{\mu}_{\mathrm{L}} &= K_{4\mathrm{L}} \Gamma_{\mathrm{L}}^{\mathrm{T}} z_{4\mathrm{L}} + \Gamma_{\mathrm{L}}^{\mathrm{T}} z_{3\mathrm{L}} + \hat{\zeta}_{\mathrm{L}} \frac{\Gamma_{\mathrm{L}}^{\mathrm{T}} z_{4\mathrm{L}} \Xi_{\mathrm{L}}^2}{\sqrt{\|z_{4\mathrm{L}}\|^2 \Xi_{\mathrm{L}}^2 + \varepsilon_{\mathrm{L}}^2}} \\ &\quad + \hat{\delta}_{2\mathrm{L}} \frac{\Gamma_{\mathrm{L}}^{\mathrm{T}} z_{4\mathrm{L}}}{\sqrt{\|z_{4\mathrm{L}}\|^2 + \varepsilon_{\mathrm{L}}^2}}. \end{aligned} \tag{28}$$

Here, $K_{4\mathrm{L}} > 0$ is a positive control gain. $\Xi_{\mathrm{L}}$ is introduced in (77). $\hat{\rho}_{J\mathrm{L}}$ is the adaptive estimate of the *unknown* lower bound $\rho_{J\mathrm{L}} = \frac{1}{J_{\mathrm{L}}}$, $\hat{\zeta}_{\mathrm{L}}$ is the adaptive estimate of the *unknown* bound $\bar{\zeta}_{\mathrm{L}}$ that is introduced in (77), and $\hat{\delta}_{2\mathrm{L}}$ is the adaptive estimate of the *unknown* bound $\bar{\delta}_{2\mathrm{L}}$ that is introduced in (76), where the adaptive laws are designed as

$$\dot{\hat{\rho}}_{J\mathrm{L}} = n_{\rho J\mathrm{L}} z_{4\mathrm{L}}^{\mathrm{T}} \Psi_{\mathrm{L}}^{\mathrm{T}} \bar{\mu}_{\mathrm{L}} - \sigma_{\rho J\mathrm{L}} \hat{\rho}_{J\mathrm{L}}, \tag{29}$$

$$\dot{\hat{\zeta}}_{\mathrm{L}} = n_{\zeta\mathrm{L}} \frac{\|z_{4\mathrm{L}}\|^2 \Xi_{\mathrm{L}}^2}{\sqrt{\|z_{4\mathrm{L}}\|^2 \Xi_{\mathrm{L}}^2 + \varepsilon_{\mathrm{L}}^2}} - \sigma_{\zeta\mathrm{L}} \hat{\zeta}_{\mathrm{L}}, \tag{30}$$

$$\dot{\hat{\delta}}_{2\mathrm{L}} = n_{\delta 2\mathrm{L}} \frac{\|z_{4\mathrm{L}}\|^2}{\sqrt{\|z_{4\mathrm{L}}\|^2 + \varepsilon_{\mathrm{L}}^2}} - \sigma_{\delta 2\mathrm{L}} \hat{\delta}_{2\mathrm{L}}, \tag{31}$$

with $n_{\rho J\mathrm{L}}$, $\sigma_{\rho J\mathrm{L}}$, $n_{\zeta\mathrm{L}}$, $\sigma_{\zeta\mathrm{L}}$, $n_{\delta 2\mathrm{L}}$, and $\sigma_{\delta 2\mathrm{L}}$ are positive adaptive gains.

Next, we design the Lyapunov function candidate as

$$V_{\mathrm{Load2}} = V_{3\mathrm{L}} + V_{4\mathrm{L}} + V_{\zeta\mathrm{L}} + V_{\rho\mathrm{L}} + V_{\delta 2\mathrm{L}}, \tag{32}$$

$$V_{\zeta\mathrm{L}} = \frac{1}{2 n_{\zeta\mathrm{L}}} \tilde{\zeta}_{\mathrm{L}}^2, \quad V_{\rho\mathrm{L}} = \frac{J_{\mathrm{L}}}{2 n_{\rho J\mathrm{L}}} \tilde{\rho}_{J\mathrm{L}}^2, \quad V_{\delta 2\mathrm{L}} = \frac{1}{2 n_{\delta 2\mathrm{L}}} \tilde{\delta}_{2\mathrm{L}}^2, \tag{33}$$

where $\tilde{\zeta}_{\mathrm{L}} = \hat{\zeta}_{\mathrm{L}} - \bar{\zeta}_{\mathrm{L}}$, $\tilde{\rho}_{J\mathrm{L}} = \hat{\rho}_{J\mathrm{L}} - \rho_{J\mathrm{L}}$ ($\rho_{J\mathrm{L}} = \frac{1}{J_{\mathrm{L}}}$), and $\tilde{\delta}_{2\mathrm{L}} = \hat{\delta}_{2\mathrm{L}} - \bar{\delta}_{2\mathrm{L}}$. The time derivative of $V_{\mathrm{Load2}}$ leads to

$$\begin{aligned} \dot{V}_{\mathrm{Load2}} &< -K_{3\mathrm{L}} z_{3\mathrm{L}}^{\mathrm{T}} z_{3\mathrm{L}} - \frac{K_{4\mathrm{L}}}{\bar{M}_{\mathrm{L}}} z_{4\mathrm{L}}^{\mathrm{T}} M_{\mathrm{L}} z_{4\mathrm{L}} - \frac{\sigma_{\zeta\mathrm{L}}}{2 n_{\zeta\mathrm{L}}} \tilde{\zeta}_{\mathrm{L}}^2 \\ &\quad - \frac{\sigma_{\rho J\mathrm{L}} J_{\mathrm{L}}}{2 n_{\rho J\mathrm{L}}} \tilde{\rho}_{J\mathrm{L}}^2 - \frac{\sigma_{\delta 2\mathrm{L}}}{2 n_{\delta 2\mathrm{L}}} \tilde{\delta}_{2\mathrm{L}}^2 + c_{2\mathrm{L}}, \end{aligned} \tag{34}$$

where $c_{2\mathrm{L}}$ is a constant and is defined as $c_{2\mathrm{L}} \triangleq \varepsilon_{\mathrm{L}}\underline{J}_{\mathrm{L}} + \varepsilon_{\mathrm{L}}(\bar{\delta}_{2\mathrm{L}} + \bar{\zeta}_{\mathrm{L}}) + \frac{\sigma_{\zeta\mathrm{L}}}{2n_{\zeta\mathrm{L}}}\bar{\zeta}_{\mathrm{L}}^2 + \frac{\sigma_{\rho J\mathrm{L}}}{2n_{\rho J\mathrm{L}}}\frac{1}{\underline{J}_{\mathrm{L}}} + \frac{\sigma_{\delta 2\mathrm{L}}}{2n_{\delta 2\mathrm{L}}}\bar{\delta}_{2\mathrm{L}}^2$.

*Step 5:*

Now we will derive the "desired cable tension" from (21) and (27), therefore we can get

$$\begin{bmatrix} T_{\mathrm{d}1}e_{\mathrm{d}1} \\ \vdots \\ T_{\mathrm{d}N}e_{\mathrm{d}N} \end{bmatrix} = P^{\mathrm{T}}\big(PP^{\mathrm{T}}\big)^{-1}\begin{bmatrix} R_{\mathrm{dL}}^{\mathrm{T}}F_{\mathrm{dL}} \\ M_{\mathrm{dL}} \end{bmatrix}, \tag{35}$$

with details presented in Appendix C (see (78)).

### B. UAV Distance Control Design

*Step 6:*

From this step onwards, we will look into the kinematics and dynamics of each UAV. At this step, we first consider the position kinematics of the quadrotors. Design the universal barrier function as

$$V_1 = \sum_{i=1}^{N}\Big(V_{\mathrm{e}i} + \sum_{j=1,j\neq i}^{N} V_{\mathrm{e}ij}\Big), \tag{36}$$

with $V_{\mathrm{e}i}$ and $V_{\mathrm{e}ij}$ defined in (16).

With algebraic analysis shown in Appendix D (see (79)–(82)), for $\dot{V}_1$ we have

$$\dot{V}_1 = \sum_{i=1}^{N}\Big\{ -\eta_{\mathrm{e}i}\xi_i - \sum_{j=1,j\neq i}^{N}\eta_{\mathrm{e}ij}\xi_{\mathrm{e}ij} + E_i^{\mathrm{T}}\dot{p}_i\Big\}, \tag{37}$$

where $\xi_i$ is introduced in (80), $\xi_{\mathrm{e}ij}$ is introduced in (82), and $E_i = [E_{xi},\ E_{yi},\ E_{zi}]^{\mathrm{T}} \in \mathbb{R}^3$ with

$$\begin{aligned} E_{xi} &= \eta_{\mathrm{e}i}\frac{\partial\eta_{\mathrm{e}i}}{\partial d_{\mathrm{e}i}}\frac{1}{d_{\mathrm{e}i}}(x_i - x_{\mathrm{d}i}) + \sum_{j=1,j\neq i}^{N} 2\eta_{\mathrm{e}ij}\frac{\partial\eta_{\mathrm{e}ij}}{\partial d_{\mathrm{e}ij}}\frac{1}{d_{ij}}(x_i - x_j), \\ E_{yi} &= \eta_{\mathrm{e}i}\frac{\partial\eta_{\mathrm{e}i}}{\partial d_{\mathrm{e}i}}\frac{1}{d_{\mathrm{e}i}}(y_i - y_{\mathrm{d}i}) + \sum_{j=1,j\neq i}^{N} 2\eta_{\mathrm{e}ij}\frac{\partial\eta_{\mathrm{e}ij}}{\partial d_{\mathrm{e}ij}}\frac{1}{d_{ij}}(y_i - y_j), \\ E_{zi} &= \eta_{\mathrm{e}i}\frac{\partial\eta_{\mathrm{e}i}}{\partial d_{\mathrm{e}i}}\frac{1}{d_{\mathrm{e}i}}(z_i - z_{\mathrm{d}i}) + \sum_{j=1,j\neq i}^{N} 2\eta_{\mathrm{e}ij}\frac{\partial\eta_{\mathrm{e}ij}}{\partial d_{\mathrm{e}ij}}\frac{1}{d_{ij}}(z_i - z_j). \end{aligned}$$

Next, define the fictitious velocity tracking error as $z_{2i} = \dot{p}_i - \alpha_{pi}$, with the stabilizing function $\alpha_{pi} \in \mathbb{R}^3$ $(i = 1, \cdots, N)$ designed as

$$\begin{aligned} \alpha_{pi} = \frac{E_i}{E_i^{\mathrm{T}}E_i}\Big\{ &-K_{\mathrm{e}i}\eta_{\mathrm{e}i}^2 - \sum_{j=1,j\neq i}^{N} K_{\mathrm{e}ij}\eta_{\mathrm{e}ij}^2 \\ &+ \eta_{\mathrm{e}i}\xi_i + \sum_{j=1,j\neq i}^{N}\eta_{\mathrm{e}ij}\xi_{\mathrm{e}ij}\Big\}, \end{aligned} \tag{38}$$

where $K_{\mathrm{e}i} > 0$ and $K_{\mathrm{e}ij} > 0$ are the control gains.

*Remark 4:* In (38), singularity can occur when $\|E_i\| = 0$. Since $\|E_i\| = 0$ if and only if $E_{xi} = 0$, $E_{yi} = 0$, and $E_{zi} = 0$ at the same time, there are two cases when this can happen. First, $\|E_i\| = 0$ when both $d_{\mathrm{e}i} = 0$ and $d_{\mathrm{e}ij} = 0$. In this situation, all the terms in the bracket on the right-hand-side of (38) are also zero, and L'Hôpital's rule we simply have $\alpha_{pi} = 0$. Second, $E_{xi} = 0$, $E_{yi} = 0$, and $E_{zi} = 0$ can happen at the same time when the position error vector $p_i - p_{\mathrm{d}i}$ and the relative position vectors $p_i - p_j$ $(j \neq i)$ are linearly dependent, which is a "deadlock situation" [30]. This situation can be bypassed by changing the reference trajectories and/or the constraint functions at the deadlock, in order to allow the vehicle breaking away from the deadlock. For the rest of discussion it is assumed that $\|E_i\| > 0$ is guaranteed.

With the controller design, (37) becomes

$$\dot{V}_1 = \sum_{i=1}^{N}\Big(E_i^{\mathrm{T}}z_{2i} - K_{\mathrm{e}i}\eta_{\mathrm{e}i}^2 - \sum_{j=1,j\neq i}^{N} K_{\mathrm{e}ij}\eta_{\mathrm{e}ij}^2\Big). \tag{39}$$

*Step 7:*

At this step, we consider the translational dynamics of the quadrotors. To address the saturation nonlinearity $\mathrm{sat}\big(F_i\big)$, the following smooth function [29] is first introduced

$$\begin{aligned} \Upsilon(F_i) &= F_{Mi}\tanh\left(\frac{F_i}{F_{Mi}}\right) \\ &= F_{Mi}\frac{\exp\big(\frac{F_i}{F_{Mi}}\big) - \exp\big(-\frac{F_i}{F_{Mi}}\big)}{\exp\big(\frac{F_i}{F_{Mi}}\big) + \exp\big(-\frac{F_i}{F_{Mi}}\big)}. \end{aligned}$$

Then, from (1), the translation dynamics of the $i$th quadrotor can be expressed as

$$\begin{aligned} \ddot{p}_i &= ge_z - \frac{1}{m_i}\mathrm{sat}(F_i)(R_{\mathrm{d}i} + R_i - R_{\mathrm{d}i})e_z + \frac{1}{m_i}T_iR_{\mathrm{L}}e_i \\ &= ge_z - \frac{1}{m_i}\Upsilon(F_i)R_{\mathrm{d}i}e_z + \frac{1}{m_i}T_iR_{\mathrm{L}}e_i - \frac{1}{m_i}\zeta_{Fi}R_{\mathrm{d}i}e_z \\ &\quad - \frac{1}{m_i}\mathrm{sat}(F_i)(R_i - R_{\mathrm{d}i})e_z, \end{aligned}$$

where $\zeta_{Fi} = \mathrm{sat}(F_i) - \Upsilon(F_i)$, which is bounded and satisfies the following condition [29]

$$|\zeta_{Fi}| = |\mathrm{sat}(F_i) - \Upsilon(F_i)| \leq F_{Mi}\big(1 - \tanh(1)\big) = d_{Fi},$$

where $d_{Fi}$ is *unknown*.

By invoking the mean value theorem [31], the function $\Upsilon(F_i)$ can be expressed as $\Upsilon(F_i) = \Upsilon(F_i^0) + \frac{\partial\Upsilon(F_i)}{\partial F_i}|_{F_i=F_i^\mu}F_i$ where $F_i^0$ is an non-negative constant and $F_i^\mu = (1-\mu)F_i^0 + \mu F_i$ with $\mu \in (0,1)$. Selecting $F_i^0 = 0$ makes $\Upsilon(F_i^0) = 0$, hence $\Upsilon(F_i) = \frac{\partial\Upsilon(F_i)}{\partial F_i}|_{F_i=F_i^\mu}F_i$.

Let $V_2 = \sum_{i=1}^{N}\frac{1}{2}z_{2i}^{\mathrm{T}}z_{2i}$, and its time derivative gives

$$\begin{aligned} \dot{V}_2 = \sum_{i=1}^{N} z_{2i}^{\mathrm{T}}\Big(&ge_z + \frac{1}{m_i}R_{\mathrm{L}}(T_{\mathrm{d}i}e_{\mathrm{d}i}^{\mathrm{T}}e_i)e_i - \dot{\alpha}_{pi} - b_{mi}u_i \\ &- \frac{1}{m_i}\mathrm{sat}(F_i)(R_i - R_{\mathrm{d}i})e_z - \frac{1}{m_i}\zeta_{Fi}R_{\mathrm{d}i}e_z \\ &+ \frac{1}{m_i}R_{\mathrm{L}}\big(T_i - (T_{\mathrm{d}i}e_{\mathrm{d}i}^{\mathrm{T}}e_i)\big)e_i\Big), \end{aligned} \tag{40}$$

where we denote $u_i = F_iR_{\mathrm{d}i}e_z$, with $R_i \triangleq R(\Theta_i)$, $R_{\mathrm{d}i} \triangleq R(\Theta_{\mathrm{d}i})$, and $b_{mi} = \frac{1}{m_i}\frac{\partial\Upsilon(F_i)}{\partial F_i}|_{F_i=F_i^\mu} = \frac{1}{m_i}\Big(1 - \tanh^2\big(\frac{F_i^\mu}{F_{Mi}}\big)\Big)$ satisfying $0 < \underline{b}_{mi} \leq b_{mi} \leq \frac{1}{m_i}$ ([31]) with $\underline{b}_{mi}$ being an *unknown* positive constant. Now, for the $i$th quadrotor

$(i = 1, \cdots, N)$, the control law $u_i \in \mathbb{R}^3$, and adaptive laws for the estimators $\hat{\bar{\delta}}_i$ and $\hat{\rho}_{mi}$ are designed as

$$u_i = \frac{z_{2i}\|\bar{u}_i\|^2\hat{\rho}_{mi}^2}{\sqrt{\|z_{2i}\|^2\|\bar{u}_i\|^2\hat{\rho}_{mi}^2 + \varepsilon_i^2}}, \tag{41}$$

$$\bar{u}_i = E_i - \dot{\alpha}_{pi} + ge_z + K_{2i}z_{2i} + \hat{\bar{\delta}}_i\frac{z_{2i}}{\sqrt{\|z_{2i}\|^2 + \varepsilon_i^2}} + \frac{1}{m_i}R_{\mathrm{L}}(T_{\mathrm{d}i}e_{\mathrm{d}i}^{\mathrm{T}}e_i)e_i, \tag{42}$$

$$\dot{\hat{\bar{\delta}}}_i = n_{\delta i}\frac{\|z_{2i}\|^2}{\sqrt{\|z_{2i}\|^2 + \varepsilon_i^2}} - \sigma_{\delta i}\hat{\bar{\delta}}_i, \tag{43}$$

$$\dot{\hat{\rho}}_{mi} = n_{\rho_{mi}}z_{2i}^{\mathrm{T}}\bar{u}_i - \sigma_{\rho_{mi}}\hat{\rho}_{mi}, \tag{44}$$

where $K_{2i} > 0$ is a control gain, $\varepsilon_i > 0$ is a design constant, $\hat{\bar{\delta}}_i$ is the estimation of the *unknown* constant $\bar{\delta}_i$ such that under Assumptions 2, 3 and the boundedness of $\zeta_{Fi}$,

$$\left\|\frac{1}{m_i}\mathrm{sat}(F_i)(R_i - R_{\mathrm{d}i})e_z\right\| + \left\|\frac{1}{m_i}R_{\mathrm{L}}\big(T_i - (T_{\mathrm{d}i}e_{\mathrm{d}i}^{\mathrm{T}}e_i)\big)e_i\right\| + \left\|\frac{1}{m_i}\zeta_{Fi}R_{\mathrm{d}i}e_z\right\| \le \bar{\delta}_i,$$

$\hat{\rho}_{mi}$ is the estimation of the *unknown* constant $\rho_{mi} = \frac{1}{\underline{b}_{mi}}$, and $n_{\delta i}$, $\sigma_{\delta i}$, $n_{\rho_{mi}}$, and $\sigma_{\rho_{mi}}$ are positive adaptive gains.

Now, choose the following Lyapunov function candidate

$$V_{\mathrm{pos}} = V_1 + V_2 + V_\delta + V_{\rho_m},$$
$$V_\delta = \sum_{i=1}^{N}\frac{1}{2n_{\delta i}}\tilde{\bar{\delta}}_i^2, \quad V_{\rho_m} = \sum_{i=1}^{N}\frac{\underline{b}_{mi}}{2n_{\rho_{mi}}}\tilde{\rho}_{mi}^2, \tag{45}$$

where $\tilde{\bar{\delta}}_i = \hat{\bar{\delta}}_i - \bar{\delta}_i$ and $\tilde{\rho}_{mi} = \hat{\rho}_{mi} - \rho_{mi}$ $(\rho_{mi} = \frac{1}{\underline{b}_{mi}})$. We can further get

$$\dot{V}_{\mathrm{pos}} < \sum_{i=1}^{N}\Bigg(-K_{\mathrm{e}i}\eta_{\mathrm{e}i}^2 - \sum_{j=1,j\neq i}^{N}K_{\mathrm{e}ij}\eta_{\mathrm{e}ij}^2 - K_{2i}z_{2i}^{\mathrm{T}}z_{2i} - \frac{\sigma_{\delta i}}{2n_{\delta i}}\tilde{\bar{\delta}}_i^2 - \frac{\underline{b}_{mi}\sigma_{\rho_{mi}}}{2n_{\rho_{mi}}}\tilde{\rho}_{mi}^2 + c_{1i}\Bigg), \tag{46}$$

where $c_{1i}$ is a constant defined as $c_{1i} \triangleq \varepsilon_i(\underline{b}_{mi} + \bar{\delta}_i) + \frac{\sigma_{\delta i}}{2n_{\delta i}}\bar{\delta}_i^2 + \frac{\sigma_{\rho_{mi}}}{2n_{\rho_{mi}}}\frac{1}{\underline{b}_{mi}}$.

Denote $V_{\mathrm{UAV1}} = V_{\mathrm{Load1}} + V_{\mathrm{Load2}} + V_{\mathrm{pos}}$, after some algebraic manipulation, we can get

$$\dot{V}_{\mathrm{UAV1}} < -\kappa_1 V_{\mathrm{UAV1}} + \varrho_1, \tag{47}$$

where

$$\kappa_1 \triangleq \min_{i,j}\Bigg(2K_{1\mathrm{L}}, \frac{2K_{2\mathrm{L}}}{M_{\mathrm{L}}}, 2K_{3\mathrm{L}}, \frac{2K_{4\mathrm{L}}}{\bar{M}_{\mathrm{L}}}, 2K_{\mathrm{e}i}, 2K_{\mathrm{e}ij}, 2K_{2i}, \sigma_{\delta 1\mathrm{L}}, \sigma_{\zeta\mathrm{L}}, \sigma_{\rho J\mathrm{L}}, \sigma_{\delta 2\mathrm{L}}, \sigma_{\delta i}, \sigma_{\rho_{mi}}\Bigg),$$

$$\varrho_1 \triangleq c_{1\mathrm{L}} + c_{2\mathrm{L}} + \sum_{i=1}^{N}c_{1i}.$$

The above backstepping design for the payload and the position of the quadrotors leads to the following results.

*Theorem 1:* With the UAV thrust laws designed as (41) and (42), and adaptive laws (22), (29), (30), (31), (43), and (44) the position control of the quadrotors and the payload described in (1) and (2) under Assumptions 1–5 have the following properties:

*i)* The user-defined constraints (11), (12), and (13) will be satisfied for $t \ge 0$.

*ii)* The transformed distance tracking errors $\eta_{\mathrm{eL}}$, $\eta_{\mathrm{e}i}$, $\eta_{\mathrm{e}ij}$, $(i = 1, \cdots, N, j \neq i)$ and attitude tracking error of payload $z_{3\mathrm{L}}$ will converge into the sets

$$\left\{x = \eta_{\mathrm{eL}}, \eta_{\mathrm{e}i}, \eta_{\mathrm{e}ij} \;\middle|\; |x| < \varepsilon_\eta,\ \varepsilon_\eta = \sqrt{\frac{2\varrho_1}{\kappa_1}}\right\}, \tag{48}$$

$$\left\{z_{3\mathrm{L}} \;\middle|\; \|z_{3\mathrm{L}}\| < \varepsilon_\eta,\ \varepsilon_\eta = \sqrt{\frac{2\varrho_1}{\kappa_1}}\right\}, \tag{49}$$

and as a result, the actual distance tracking errors $d_{\mathrm{eL}}$, $d_{\mathrm{e}i}$, and $d_{\mathrm{e}ij}$ will converge to the sets

$$\left\{x = d_{\mathrm{eL}}, d_{\mathrm{e}i} \;\middle|\; x < \varepsilon_{\chi\mathrm{H},i}\right\}, \tag{50}$$

$$\left\{d_{\mathrm{e}ij} \;\middle|\; -\varepsilon_{\iota\mathrm{W},i} < d_{\mathrm{e}ij} < \varepsilon_{\iota\mathrm{H},i}\right\}, \tag{51}$$

where

$$\varepsilon_{\chi\mathrm{H},i} = \frac{\varepsilon_\eta\Omega_{d\mathrm{H}i}}{\Omega_{d\mathrm{H}i} + \varepsilon_\eta}, \tag{52}$$

and we have $\varepsilon_{\iota\mathrm{H},i}$ expressed in (53), with $\varepsilon_{\iota\mathrm{W},i}$ expressed in (54), shown at the bottom of the next page, where $\Omega_{\mathrm{H}} = \Omega_{\mathrm{H}ij}$ and $\Omega_{\mathrm{W}} = \Omega_{\mathrm{W}ij}$ for $i, j = 1, \cdots, N$, $j \neq i$.

*iii)* The control laws as (41) and (42), and adaptive laws (22), (29), (30), (31), (43), and (44) are all uniformly bounded.

*Proof:* See Appendix E. ∎

*Remark 5:* In Theorem 1, using L'Hôpital's rule we get

$$\lim_{\varepsilon_\eta\to 0}\varepsilon_{\iota\mathrm{H},i} = 0, \quad \lim_{\varepsilon_\eta\to 0}\varepsilon_{\iota\mathrm{W},i} = 0, \quad \lim_{\varepsilon_\eta\to 0}\varepsilon_{\chi\mathrm{H},i} = 0 \tag{55}$$

for $i = 1, \cdots, N$. This implies that the transformed error variables $\eta_{\mathrm{eL}}$, $\eta_{\mathrm{e}i}$, and $\eta_{\mathrm{e}ij}$, converge into small neighbourhoods of zero, so does the actual distance tracking errors $d_{\mathrm{eL}}$, $d_{\mathrm{e}i}$, and $d_{\mathrm{e}ij}$.

*Remark 6:* To reduce the size of the set in (48) and (49), we need to select large $\kappa_1$ and small $\varrho_1$. To make $\kappa_1$ large, we can select large control gains $K_{1\mathrm{L}}$, $K_{2\mathrm{L}}$, $K_{3\mathrm{L}}$, $K_{4\mathrm{L}}$, $K_{\mathrm{e}i}$, $K_{\mathrm{e}ij}$, and $K_{2i}$ for $i, j = 1, \cdots, N$, $j \neq i$, and large adaptive control parameters $\sigma_{\delta 1\mathrm{L}}$, $\sigma_{\zeta\mathrm{L}}$, $\sigma_{\rho J\mathrm{L}}$, $\sigma_{\delta 2\mathrm{L}}$, $\sigma_{\delta i}$, and $\sigma_{\rho_{mi}}$, for $i = 1, \cdots, N$. To make $\varrho_1$ small, we can select small $\varepsilon_{\mathrm{L}}$ and $\varepsilon_i$, and large adaptive control parameters $n_{\delta 1\mathrm{L}}$, $n_{\zeta\mathrm{L}}$, $n_{\rho J\mathrm{L}}$, $n_{\delta 2\mathrm{L}}$, $n_{\delta i}$, and $n_{\rho_{mi}}$.

### C. UAV Attitude Control Design

*Step 8:*

Here we consider the attitude kinematics of the quadrotors. Define $z_{3i} = \Theta_i - \Theta_{\mathrm{d}i}$ and $z_{4i} = \dot{\Theta}_i - \alpha_{\Theta i}$, where $\Theta_{\mathrm{d}i}$ is shown in Appendix F and $\alpha_{\Theta i}$ is a stabilizing function designed as

$$\alpha_{\Theta i} = -\Big(K_{3i} + \frac{\nu_i}{2}\Big)z_{3i}, \tag{56}$$

$$\varepsilon_{\iota\mathrm{H},i} = \frac{\varepsilon_\eta\Omega_{d\mathrm{H}i}}{\Omega_{d\mathrm{H}i} - \varepsilon_\eta}, \quad \varepsilon_{\iota\mathrm{W},i} = \frac{\varepsilon_\eta\Omega_{d\mathrm{W}i}}{\Omega_{d\mathrm{W}i} - \varepsilon_\eta} \tag{53, 54}$$

with $K_{3i}$ and $\nu_i$ being a positive control gain and a positive design constant, respectively. Now, design the Lyapunov candidate as $V_3 = \sum_{i=1}^{N} \frac{1}{2} z_{3i}^{\mathrm{T}} z_{3i}$, its derivative gives rise to

$$\dot{V}_3 \leq \sum_{i=1}^{N} \Big( - K_{3i} z_{3i}^{\mathrm{T}} z_{3i} + z_{3i}^{\mathrm{T}} z_{4i} + \frac{1}{2\nu_i} \bar{\Theta}_{\mathrm{d}i}^2 \Big). \tag{57}$$

Details including the definition of $\bar{\Theta}_{\mathrm{d}i}$ can be seen in Appendix F.

*Step 9:*

Now, choose the Lyapunov function candidate as $V_4 = \sum_{i=1}^{N} \frac{1}{2} z_{4i}^{\mathrm{T}} M_i z_{4i}$. With some algebric analysis shown in Appendix G (see (88)–(89)), design the control law for the $i$th UAV as

$$\tau_i = - \frac{\Psi_i z_{4i} \| \bar{\tau}_i \|^2 \hat{\rho}_{Ji}^2}{\sqrt{\| \Psi_i z_{4i} \|^2 \| \bar{\tau}_i \|^2 \hat{\rho}_{Ji}^2 + \varepsilon_i^2}}, \tag{58}$$

$$\bar{\tau}_i = K_{4i} \Gamma_i^{\mathrm{T}} z_{4i} + \Gamma_i^{\mathrm{T}} z_{3i} + \hat{\zeta}_i \frac{\Gamma_i^{\mathrm{T}} z_{4i} \Xi_i^2}{\sqrt{\| z_{4i} \|^2 \Xi_i^2 + \varepsilon_i^2}}, \tag{59}$$

$$\dot{\hat{\rho}}_{Ji} = n_{\rho Ji} z_{4i}^{\mathrm{T}} \Psi_i^{\mathrm{T}} \bar{\tau}_i - \sigma_{\rho Ji} \hat{\rho}_{Ji}, \tag{60}$$

$$\dot{\hat{\zeta}}_i = n_{\zeta i} \frac{\| z_{4i} \|^2 \Xi_i^2}{\sqrt{\| z_{4i} \|^2 \Xi_i^2 + \varepsilon_i^2}} - \sigma_{\zeta i} \hat{\zeta}_i, \tag{61}$$

where $K_{4i} > 0$ is a positive control gain. $\Xi_i$ is introduced in (89). $\hat{\rho}_{Ji}$ is the adaptive estimate of the *unknown* constant $\rho_{Ji} = \frac{1}{\underline{J}_i}$, and $\hat{\zeta}_i$ is the adaptive estimate of the *unknown* constant $\zeta_i$ that is introduced in (89). $n_{\rho Ji}$, $\sigma_{\rho Ji}$, $n_{\zeta i}$, and $\sigma_{\zeta i}$ are positive adaptive gains. Denote

$$\begin{aligned} V_{\mathrm{att}} &= V_3 + V_4 + V_\zeta + V_\rho, \\ V_\zeta &= \sum_{i=1}^{N} \frac{1}{2 n_{\zeta i}} \tilde{\zeta}_i^2, \quad V_\rho = \sum_{i=1}^{N} \frac{\underline{J}_i}{2 n_{\rho Ji}} \tilde{\rho}_{Ji}^2, \end{aligned} \tag{62}$$

where $\tilde{\zeta}_i = \hat{\zeta}_i - \bar{\zeta}_i$ and $\tilde{\rho}_{Ji} = \hat{\rho}_{Ji} - \rho_{Ji}$. After some algebraic manipulation, we can arrive at

$$\begin{aligned} \dot{V}_{\mathrm{att}} < \sum_{i=1}^{N} \Big( & - K_{3i} z_{3i}^{\mathrm{T}} z_{3i} - \frac{K_{4i}}{\bar{M}_i} z_{4i}^{\mathrm{T}} M_i z_{4i} - \frac{\sigma_{\zeta i}}{2 n_{\zeta i}} \tilde{\zeta}_i^2 \\ & - \frac{\sigma_{\rho Ji} \underline{J}_i}{2 n_{\rho Ji}} \tilde{\rho}_{Ji}^2 + c_{2i} \Big), \end{aligned} \tag{63}$$

where $c_{2i}$ is a constant and is defined as $c_{2i} = \varepsilon_i (\underline{J}_i + \bar{\zeta}_i) + \frac{\sigma_{\zeta i}}{2 n_{\zeta i}} \bar{\zeta}_i^2 + \frac{\sigma_{\rho Ji}}{2 n_{\rho Ji}} \frac{1}{\underline{J}_i} + \frac{1}{2\nu_i} \bar{\Theta}_{\mathrm{d}i}^2$.

Hence, let the Lyapunov function for the attitude part of the quadrotor be $V_{\mathrm{UAV2}} = V_{\mathrm{att}}$, we can get

$$\dot{V}_{\mathrm{UAV2}} < - \kappa_2 V_{\mathrm{UAV2}} + \varrho_2, \tag{64}$$

where

$$\kappa_2 \triangleq \min_i \Big( 2K_{3i}, \frac{2K_{4i}}{\bar{M}_i}, \sigma_{\zeta i}, \sigma_{\rho Ji} \Big), \quad \varrho_2 \triangleq \sum_{i=1}^{N} c_{2i}.$$

The above backstepping design for the attitude part of UAVs leads to the following theoretical result.

*Theorem 2:* With the UAV torque laws as (58) and (59), and adaptive laws (60) and (61), the attitude control of the quadrotor system described by (1) under Assumptions 1–5 has the following properties:

*i)* The attitude tracking error of the quadrotor $z_{3i}$ ($i = 1, \cdots, N$) will converge into the set

$$\left\{ z_{3i} \;\middle|\; \| z_{3i} \| < \varepsilon_\eta, \ \varepsilon_\eta = \sqrt{\frac{2\varrho_2}{\kappa_2}} \right\}, \tag{65}$$

*ii)* The torque laws (58) and (59), and adaptive laws (60) and (61) are all uniformly bounded.

*Proof:* See Appendix H. ∎

*Remark 7:* To reduce the set size in (65), large $\kappa_2$ and small $\varrho_2$ can be selected. To make $\kappa_2$ large, we can select large control gains $K_{3i}$ and $K_{4i}$ for $i = 1, \cdots, N$, and large adaptive control parameters $\sigma_{\zeta i}$ and $\sigma_{\rho Ji}$ for $i = 1, \cdots, N$. To make $\varrho_2$ small, we can select small $\varepsilon_i$, and large adaptive control parameters $n_{\zeta i}$ and $n_{\rho Ji}$ for $i = 1, \cdots, N$.

*Remark 8:* Once the thrust and torque of the $i$th quadrotor ($i = 1, \cdots, N$) are determined, the propeller speeds can be calculated using the following relation

$$\begin{bmatrix} F_i \\ \tau_{\phi i} \\ \tau_{\theta i} \\ \tau_{\psi i} \end{bmatrix} = \begin{bmatrix} \upsilon_i & \upsilon_i & \upsilon_i & \upsilon_i \\ 0 & -l_i \upsilon_i & 0 & l_i \upsilon_i \\ -l_i \upsilon_i & 0 & l_i \upsilon_i & 0 \\ \iota_i & -\iota_i & \iota_i & -\iota_i \end{bmatrix} \begin{bmatrix} \omega_{\mathrm{roti}1}^2 \\ \omega_{\mathrm{roti}2}^2 \\ \omega_{\mathrm{roti}3}^2 \\ \omega_{\mathrm{roti}4}^2 \end{bmatrix},$$

where $F_i \in \mathbb{R}^+$ is subject to saturation, $\tau_i = [\tau_{\phi i}, \ \tau_{\theta i}, \ \tau_{\psi i}]^{\mathrm{T}} \in \mathbb{R}^3$. $\omega_{\mathrm{roti}1}$, $\omega_{\mathrm{roti}2}$, $\omega_{\mathrm{roti}3}$, and $\omega_{\mathrm{roti}4}$ represent the front, right, rear, and left propeller speeds of the $i$th quadrotor, respectively. $l_i$ is the distance between the center of the propeller and the center of the $i$th quadrotor, $\upsilon_i$ is a thrust factor of the $i$th quadrotor, and $\iota_i$ is a drag factor of the $i$th quadrotor ($i = 1, \cdots, N$).

The overall control algorithm can be summarized into the following block diagram (Figure 3).

## V. Simulation Studies

In this section, a simulation example is carried out with a team of $N = 4$ quadrotors and an irregular payload. The model parameters of the quadrotors are $m_i = 1\mathrm{kg}$, $g = 9.81\mathrm{m/s}^2$, $J_i = \mathrm{diag}[0.109, \ 0.103, \ 0.0625]\mathrm{kg} \cdot \mathrm{m}^2$, and $F_{Mi} = 75\mathrm{N}$, $i = 1, 2, 3, 4$. The mass and inertia matrix of the payload

$$\varepsilon_{\iota_{\mathrm{H},i}} = \frac{-(\Omega_{\mathrm{H}}\Omega_{\mathrm{W}} - \varepsilon_\eta(\Omega_{\mathrm{H}} - \Omega_{\mathrm{W}})) + \sqrt{\Omega_{\mathrm{H}}^2\Omega_{\mathrm{W}}^2 + \varepsilon_\eta^2(\Omega_{\mathrm{H}} + \Omega_{\mathrm{W}})^2 - 2\varepsilon_\eta\Omega_{\mathrm{H}}\Omega_{\mathrm{W}}(\Omega_{\mathrm{H}} - \Omega_{\mathrm{W}})}}{2\varepsilon_\eta}, \tag{53}$$

$$\varepsilon_{\iota_{\mathrm{W},i}} = \frac{-(\Omega_{\mathrm{H}}\Omega_{\mathrm{W}} + \varepsilon_\eta(\Omega_{\mathrm{H}} - \Omega_{\mathrm{W}})) + \sqrt{\Omega_{\mathrm{H}}^2\Omega_{\mathrm{W}}^2 + \varepsilon_\eta^2(\Omega_{\mathrm{H}} + \Omega_{\mathrm{W}})^2 + 2\varepsilon_\eta\Omega_{\mathrm{H}}\Omega_{\mathrm{W}}(\Omega_{\mathrm{H}} - \Omega_{\mathrm{W}})}}{2\varepsilon_\eta}. \tag{54}$$

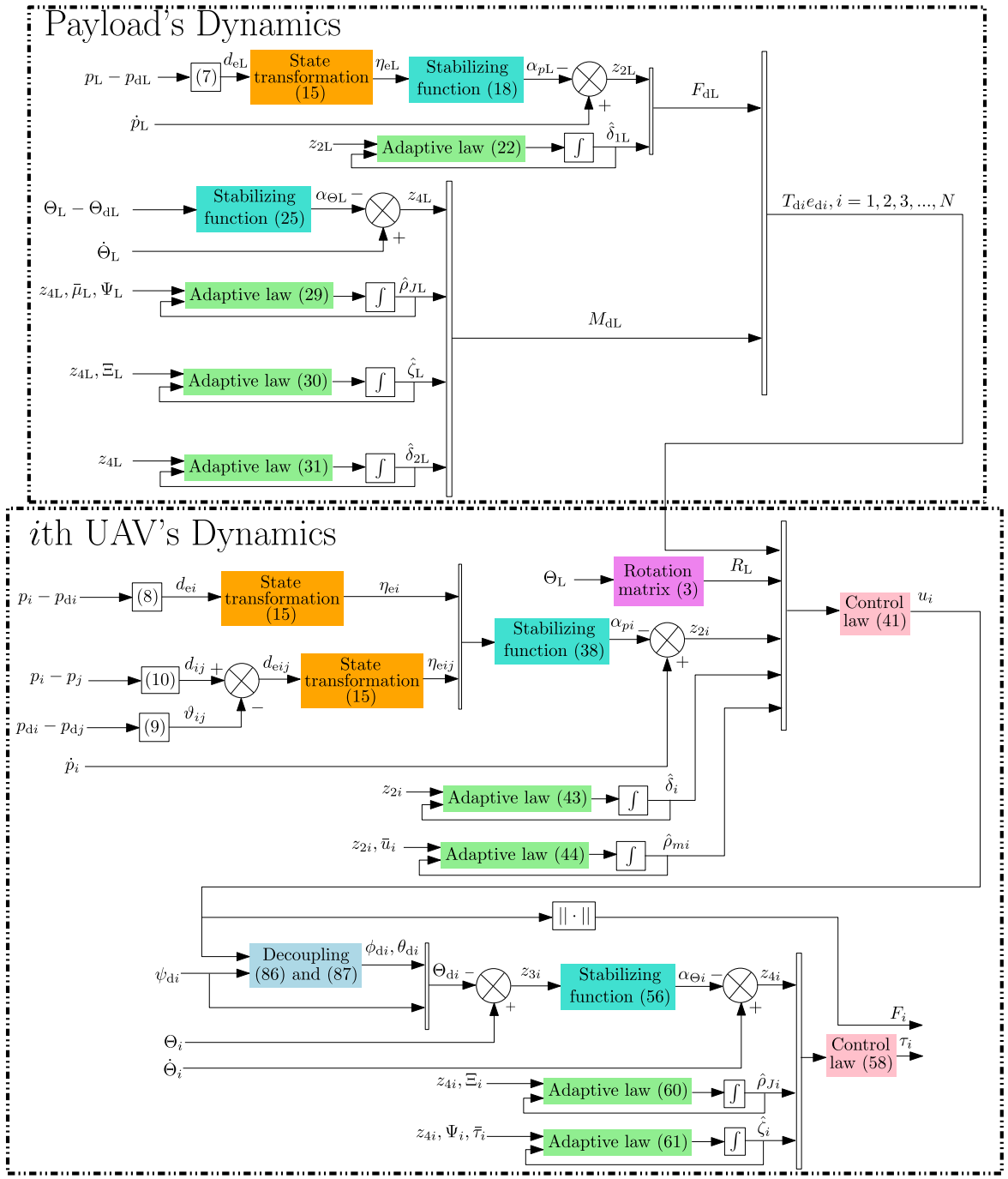


Fig. 3. Block diagram of the overall control algorithm.

are $m_{\rm L}=2$kg and $J_{\rm L}=\text{diag}[0.095,\ 0.14,\ 0.2388]\text{kg}\cdot\text{m}^2$, respectively. Note that $J_i$ and $J_{\rm L}$ are unknown to the controller design. The length of cables is $l_i=2.5$m, $i=1,2,3,4$, and they are attached to the points of the payload $r_1=[0.25,\ -0.2,\ -0.45]^{\rm T}$, $r_2=[-0.5,\ -0.4,\ -0.15]^{\rm T}$, $r_3=[-0.5,\ 0.4,\ 0.15]^{\rm T}$, and $r_4=[0.5,\ 0.4,\ 0]^{\rm T}$. Note that the units of the position, attitude, translational and angular velocities are m, rad, m/s, and rad/s, respectively. The desired trajectory of the payload is selected as $p_{\rm dL}(t)=[x_{\rm dL}(t),\ y_{\rm dL}(t),\ z_{\rm dL}(t)]^{\rm T}=[0.2t-0.35,\ 3.5\sin(0.15t),\ -0.2t+0.01\sin(25t)-1.5]^{\rm T}$. The desired attitude of the payload is $\Theta_{\rm dL}=[0,\ 0,\ 0]^{\rm T}$. Next, the desired unit direction vector from the mass center of the $i$th UAV towards the $i$th link attachment point is selected as $e_{{\rm d}i}(t)=[e_{{\rm d}i1}(t),\ e_{{\rm d}i2}(t),\ e_{{\rm d}i3}(t)]^{\rm T}$ where $e_{{\rm d}i1}(t)=\varphi_i\frac{x_{\rm dL}(t)-x_{\rm dL}(t+\varpi_{{\rm dL}i})}{\|p_{\rm dL}(t)-p_{\rm dL}(t+\varpi_{{\rm dL}i})\|}$, $e_{{\rm d}i2}(t)=\varphi_i\frac{y_{\rm dL}(t)-y_{\rm dL}(t+\varpi_{{\rm dL}i})}{\|p_{\rm dL}(t)-p_{\rm dL}(t+\varpi_{{\rm dL}i})\|}$, $e_{{\rm d}i3}(t)=\sqrt{1-\varphi_i^2+\varphi_i^2\frac{|z_{\rm dL}(t)-z_{\rm dL}(t+\varpi_{{\rm dL}i})|^2}{\|p_{\rm dL}(t)-p_{\rm dL}(t+\varpi_{{\rm dL}i})\|}}$, $\varphi_i=0.35$, and $\varpi_{{\rm dL}i}=2$, $i=1,2,3,4$. Thus, the desired trajectory of the $i$th UAV can be written as $p_{\rm di}=p_{\rm dL}+R(\Theta_{\rm dL})r_i-l_ie_{{\rm d}i}$. Besides, the desired yaw angle of the $i$th UAV is selected as $\psi_{\rm di}=0$, $i=1,2,3,4$. Moreover, the constraint functions are selected as $\Omega_{d{\rm H}i}=(7.8-0.2)e^{-0.4t}+0.2$, $\Omega_{d{\rm HL}}=(7.8-0.2)e^{-0.4t}+0.2$, $\Omega_{{\rm H}ij}=(2-0.1)e^{-0.1t}+0.1$, and $\Omega_{{\rm W}ij}=(1.8-0.1)e^{-0.15t}+0.1$, $i,j=1,2,3,4, i\neq j$.

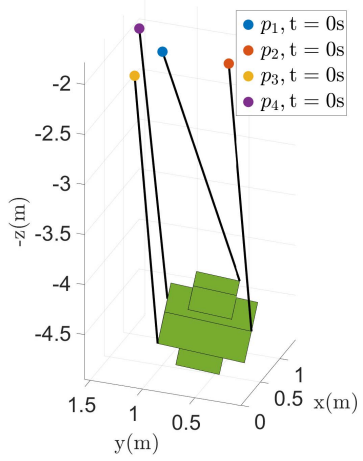


Fig. 4. Initial conditions of the load and quadrotors in 3D space at $t = 0$.

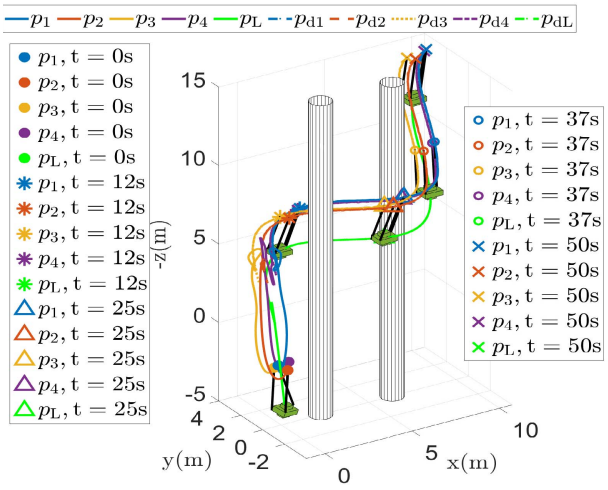


Fig. 5. Trajectories of the quadrotors and the load in 3D space.

To implement the proposed control framework, the design parameters are chosen as $n_{\delta 1\mathrm{L}} = 0.25$, $n_{\rho J\mathrm{L}} = 0.25$, $n_{\zeta\mathrm{L}} = 0.25$, $n_{\delta 2\mathrm{L}} = 0.25$, $\sigma_{\delta 1\mathrm{L}} = 0.1$, $\sigma_{\rho J\mathrm{L}} = 0.1$, $\sigma_{\zeta\mathrm{L}} = 0.1$, $\sigma_{\delta 2\mathrm{L}} = 0.1$, $\varepsilon_{\mathrm{L}} = 0.1$, $\varepsilon_i = 0.1$, $n_{\delta i} = 0.15$, $n_{\rho Ji} = 0.15$, $n_{\zeta i} = 0.15$, $n_{\rho mi} = 0.1$, $\sigma_{\delta i} = 0.05$, $\sigma_{\rho Ji} = 0.05$, $\sigma_{\zeta i} = 0.05$, $\sigma_{\rho mi} = 0.01$, and $i = 1, 2, 3, 4$. The control gains are designed as $K_{1\mathrm{L}} = 3.55$, $K_{2\mathrm{L}} = 3.55$, $K_{3\mathrm{L}} = 2.35$, $K_{4\mathrm{L}} = 2.35$, $K_{ei} = 3.15$, $K_{eij} = 0.45$, $K_{vi} = 3.15$, $v_i = 0.5$, $K_{\Theta i} = 0.75$, and $K_{\omega i} = 1.2$, $i = 1, 2, 3, 4$.

The initial position and attitude of the payload are $p_{\mathrm{L}}(0) = [0.6,\ 0.6,\ 4.5]^{\mathrm{T}}$ and $\Theta_{\mathrm{L}}(0) = [-0.2,\ -0.2,\ 0.3]^{\mathrm{T}}$, respectively. Thus, the initial position of the $i$th UAV can be expressed as $p_i(0) = p_{\mathrm{L}}(0) + R\big(\Theta_{\mathrm{L}}(0)\big)\rho_i - l_i e_i(0)$, where $e_1(0) = [0.2208,\ -0.2208,\ 0.95]^{\mathrm{T}}$, $e_2(0) = [-0.1407,\ 0.1407,\ 0.98]^{\mathrm{T}}$, $e_3(0) = [-0.1407,\ -0.1407,\ 0.98]^{\mathrm{T}}$, $e_4(0) = [-0.1719,\ -0.1719,\ 0.97]^{\mathrm{T}}$, and the initial attitude of the $i$th UAV is $\Theta_i(0) = [0,\ 0,\ 0.3]^{\mathrm{T}}$, $i = 1, 2, 3, 4$. The initial positions of quadrotors and the payload in 3D space are recorded in Figure 4 to show the shape of this irregular payload, the initial attitude of the payload, the cable connection locations, and the initial positions of UAVs. The initial conditions of the translational and angular velocities of every UAV and the payload are zero.

The simulation results are presented in Figures 5-10. The 3D trajectories of four quadrotors and one payload are depicted in Figure 5. A YouTube video for the simulation process can also be viewed at: `https://youtu.be/XrKB_DVq3DU` (To view the video, copy and paste the complete URL to a web browser). It can be observed that the quadrotors and payload can track the desired $N$-shaped paths around two obstacles represented by cylinders. The LOS distance tracking errors $d_{\mathrm{e}i}$ and $d_{\mathrm{eL}}$ under the proposed controller are shown in Figure 6 with $\Omega_{d\mathrm{H}i}$ and $\Omega_{d\mathrm{HL}}$, $i = 1, 2, 3, 4$. From this figure, we see that $d_{\mathrm{e}i}$ and $d_{\mathrm{eL}}$ can converge to small neighborhoods of the origin without violation of the performance constraints $\Omega_{d\mathrm{H}i}$ and $\Omega_{d\mathrm{HL}}$, respectively. Figure 7 gives the profile of the inter-quadrotor distance tracking errors $d_{\mathrm{e}ij}$ under the proposed controller, $i, j = 1, 2, 3, 4$, $j \neq i$. It is clear that the safety constraint requirements are met during the

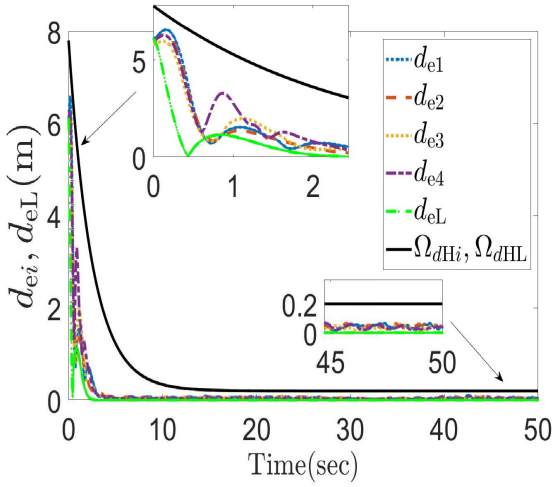


Fig. 6. The profile of the LOS distance tracking errors $d_{\mathrm{e}i}$ with $\Omega_{d\mathrm{H}i}$, $i = 1, 2, 3, 4$, and $d_{\mathrm{eL}}$ with $\Omega_{d\mathrm{HL}}$.

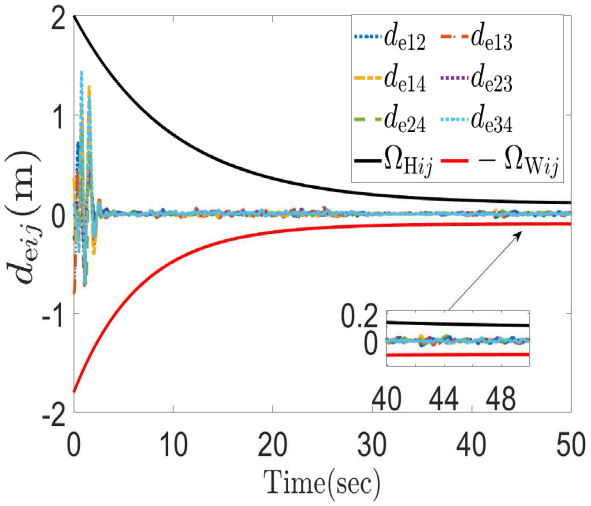


Fig. 7. The profile of the relative inter-quadrotor distance tracking errors $d_{\mathrm{e}ij}$ with $\Omega_{\mathrm{H}ij}$ and $-\Omega_{\mathrm{W}ij}$, $i, j = 1, 2, 3, 4$, $i \neq j$.

cooperative transportation operation since $d_{\mathrm{e}ij}$ always stays between the constraint functions, $-\Omega_{\mathrm{W}ij}$ and $\Omega_{\mathrm{H}ij}$. The profile

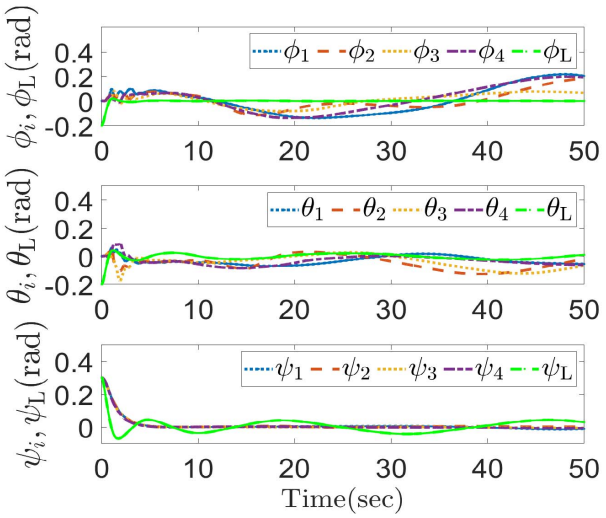


Fig. 8. The profile of the attitudes of the payload and the quadrotors, $\phi_L$, $\theta_L$, $\psi_L$, $\phi_i$, $\theta_i$, and $\psi_i$, $i = 1, 2, 3, 4$.

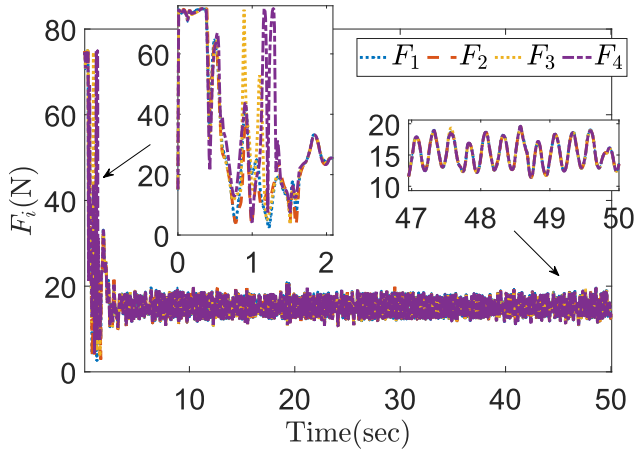


Fig. 9. The thrust $F_i$ of quadrotors, $i = 1, 2, 3, 4$.

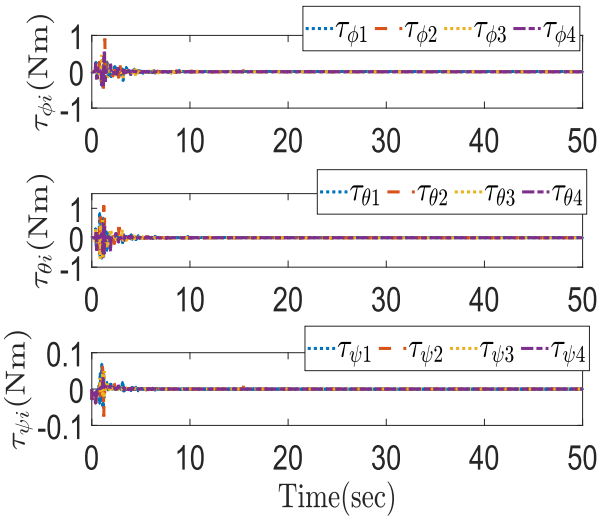


Fig. 10. Torques $\tau_{\phi i}, \tau_{\theta i}, \tau_{\psi i}$ of quadrotors, $i = 1, 2, 3, 4$.

of the attitudes of the payload and quadrotors, $\phi_L$, $\theta_L$, $\psi_L$, $\phi_i$, $\theta_i$, and $\psi_i$, $i = 1, 2, 3, 4$, presented in Figure 8 shows that the convergence of the attitudes to their own desired values despite the lack of model parameters. The thrust $F_i$ subject to saturation and the torques of $\phi_i$, $\theta_i$ and $\psi_i$, $i = 1, 2, 3, 4$, are plotted in Figure 9 and 10, respectively. The sum of thrusts provided by every quadrotor can make this cable-suspended cooperative system track the reference trajectory with desired acceleration. The torques can stabilize the attitude of quadrotors and make the payload to track its desired angles despite the lack of accurate model parameters. From the aforementioned discussion, we can now conclude that the simulation results align with the theoretical results discussed in Theorem 1 and 2.

## VI. Concluding Remarks

In this paper, we propose a new constrained cooperative control architecture for load transportation by a group of UAVs. Multiple user-defined time-varying system constraint requirements on performance and safety during the operation are dealt with by the universal barrier function structures. Control saturation and uncertainties in UAV inertia matrices are dealt with by employing adaptive estimators. Exponential convergence of the distance and attitude tracking errors can be guaranteed. Future research includes experiment verification of the framework, and mitigation of measurement noise and environment disturbances during cooperative load transportation tasks.

## Appendix

### A. System Dynamics

Denote

$$\Psi(\Theta_i) = \Gamma^{-1}(\Theta_i), \tag{66}$$

from (1) we get

$$\omega_i = \Psi(\Theta_i)\dot{\Theta}_i. \tag{67}$$

Hence, multiply $J_i^{\mathrm{T}}$ on both sides of the third equation in (1), and substitute (67) into the third equation in (1), the angular motion dynamics of the UAV can be rewritten as

$$J_i^{\mathrm{T}} J_i \Big(\Psi(\Theta_i)\ddot{\Theta}_i + \dot{\Psi}(\Theta_i)\dot{\Theta}_i\Big) + J_i^{\mathrm{T}} \mathbb{S}\Big(\Psi(\Theta_i)\dot{\Theta}_i\Big) J_i \Psi(\Theta_i)\dot{\Theta}_i = J_i^{\mathrm{T}} \tau_i. \tag{68}$$

Now, multiply $\Psi^{\mathrm{T}}(\Theta_i)$ on both sides of (68), we can get

$$M_i(\Theta_i)\ddot{\Theta}_i + C_i(\Theta_i, \dot{\Theta}_i)\dot{\Theta}_i = \Psi^{\mathrm{T}}(\Theta_i) J_i^{\mathrm{T}} \tau_i, \tag{69}$$

where

$$M_i(\Theta_i) = \Psi^{\mathrm{T}}(\Theta_i) J_i^{\mathrm{T}} J_i \Psi(\Theta_i), \tag{70}$$

$$C_i(\Theta_i, \dot{\Theta}_i) = \Psi^{\mathrm{T}}(\Theta_i) J_i^{\mathrm{T}} \mathbb{S}\Big(\Psi(\Theta_i)\dot{\Theta}_i\Big) J_i \Psi(\Theta_i) + \Psi^{\mathrm{T}}(\Theta_i) J_i^{\mathrm{T}} J_i \dot{\Psi}(\Theta_i). \tag{71}$$

It is easy to verify that $M_i(\Theta_i)$ is symmetric and positive definite, and for any $x \in \mathbb{R}^3$,

$$x^{\mathrm{T}}\Big(\dot{M}_i(\Theta_i) - 2C_i(\Theta_i, \dot{\Theta}_i)\Big)x = 0.$$

In a similar way, for the payload we can also obtain

$$M_{\mathrm{L}}(\Theta_{\mathrm{L}})\ddot{\Theta}_{\mathrm{L}} + C_{\mathrm{L}}(\Theta_{\mathrm{L}}, \dot{\Theta}_{\mathrm{L}})\dot{\Theta}_{\mathrm{L}} = \Psi^{\mathrm{T}}(\Theta_{\mathrm{L}})J_{\mathrm{L}}^{\mathrm{T}}\sum_{i=1}^{N}\mathbb{S}(r_i)(-T_i e_i), \tag{72}$$

where

$$M_{\mathrm{L}}(\Theta_{\mathrm{L}}) = \Psi^{\mathrm{T}}(\Theta_{\mathrm{L}})J_{\mathrm{L}}^{\mathrm{T}}J_{\mathrm{L}}\Psi(\Theta_{\mathrm{L}}), \tag{73}$$

$$C_{\mathrm{L}}(\Theta_{\mathrm{L}}, \dot{\Theta}_{\mathrm{L}}) = \Psi^{\mathrm{T}}(\Theta_{\mathrm{L}})J_{\mathrm{L}}^{\mathrm{T}}\mathbb{S}\Big(\Psi(\Theta_{\mathrm{L}})\dot{\Theta}_{\mathrm{L}}\Big)J_{\mathrm{L}}\Psi(\Theta_{\mathrm{L}}) + \Psi^{\mathrm{T}}(\Theta_{\mathrm{L}})J_{\mathrm{L}}^{\mathrm{T}}J_{\mathrm{L}}\dot{\Psi}(\Theta_{\mathrm{L}}). \tag{74}$$

### B. Step 4 of Backstepping Design

Taking derivative of $V_{4\mathrm{L}}$ leads to

$$\begin{aligned}\dot{V}_{4\mathrm{L}} &= \frac{1}{2}z_{4\mathrm{L}}^{\mathrm{T}}\dot{M}_{\mathrm{L}}z_{4\mathrm{L}} + z_{4\mathrm{L}}^{\mathrm{T}}\Big(M_{\mathrm{L}}\ddot{\Theta}_{\mathrm{L}} - M_{\mathrm{L}}\dot{\alpha}_{\Theta\mathrm{L}}\Big)\\ &= z_{4\mathrm{L}}^{\mathrm{T}}\Big(\Psi_{\mathrm{L}}^{\mathrm{T}}J_{\mathrm{L}}^{\mathrm{T}}\sum_{i=1}^{N}\mathbb{S}(r_i)(T_{\mathrm{d}i}e_{\mathrm{d}i} - T_i e_i)\\ &\quad + \Psi_{\mathrm{L}}^{\mathrm{T}}J_{\mathrm{L}}^{\mathrm{T}}\sum_{i=1}^{N}\mathbb{S}(r_i)(-T_{\mathrm{d}i}e_{\mathrm{d}i}) - M_{\mathrm{L}}\dot{\alpha}_{\Theta\mathrm{L}} - C_{\mathrm{L}}\alpha_{\Theta\mathrm{L}}\Big),\end{aligned} \tag{75}$$

where $\frac{1}{2}z_{4\mathrm{L}}^{\mathrm{T}}(\dot{M}_{\mathrm{L}} - 2C_{\mathrm{L}})z_{4\mathrm{L}} = 0$. Under Assumption 2 and Lemma 1, from (75) we have

$$\begin{aligned}&z_{4\mathrm{L}}^{\mathrm{T}}\Psi_{\mathrm{L}}^{\mathrm{T}}J_{\mathrm{L}}^{\mathrm{T}}\sum_{i=1}^{N}\mathbb{S}(r_i)(T_{\mathrm{d}i}e_{\mathrm{d}i} - T_i e_i)\\ &\quad\le \|z_{4\mathrm{L}}\|\bar{\delta}_{2\mathrm{L}} < \varepsilon_{\mathrm{L}}\bar{\delta}_{2\mathrm{L}} + \bar{\delta}_{2\mathrm{L}}\frac{\|z_{4\mathrm{L}}\|^2}{\sqrt{\|z_{4\mathrm{L}}\|^2 + \varepsilon_{\mathrm{L}}^2}},\end{aligned} \tag{76}$$

where $\bar{\delta}_{2\mathrm{L}} > 0$ is an *unknown* constant bound. Furthermore, using the notation definitions in (73), we can obtain the following

$$\begin{aligned}&z_{4\mathrm{L}}^{\mathrm{T}}(-M_{\mathrm{L}}\dot{\alpha}_{\Theta\mathrm{L}} - C_{\mathrm{L}}\alpha_{\Theta\mathrm{L}})\\ &\quad= -z_{4\mathrm{L}}^{\mathrm{T}}\Psi_{\mathrm{L}}^{\mathrm{T}}J_{\mathrm{L}}^{\mathrm{T}}J_{\mathrm{L}}\Big(\Psi_{\mathrm{L}}\dot{\alpha}_{\Theta\mathrm{L}} + \dot{\Psi}_{\mathrm{L}}\alpha_{\Theta\mathrm{L}}\Big)\\ &\qquad - z_{4\mathrm{L}}^{\mathrm{T}}\Psi_{\mathrm{L}}^{\mathrm{T}}J_{\mathrm{L}}^{\mathrm{T}}\mathbb{S}(\Psi_{\mathrm{L}}\dot{\Theta}_{\mathrm{L}})J_{\mathrm{L}}\Psi_{\mathrm{L}}\alpha_{\Theta\mathrm{L}}\\ &\quad\le \|z_{4\mathrm{L}}\|\|\Psi_{\mathrm{L}}\|\|J_{\mathrm{L}}\|^2\Big(\|\Psi_{\mathrm{L}}\dot{\alpha}_{\Theta\mathrm{L}} + \dot{\Psi}_{\mathrm{L}}\alpha_{\Theta\mathrm{L}}\|\\ &\qquad + \|\mathbb{S}(\Psi_{\mathrm{L}}\dot{\Theta}_{\mathrm{L}})\|\|\Psi_{\mathrm{L}}\alpha_{\Theta\mathrm{L}}\|\Big)\\ &\quad< \varepsilon_{\mathrm{L}}\bar{\zeta}_{\mathrm{L}} + \bar{\zeta}_{\mathrm{L}}\frac{\|z_{4\mathrm{L}}\|^2\Xi_{\mathrm{L}}{}^2}{\sqrt{\|z_{4\mathrm{L}}\|^2\Xi_{\mathrm{L}}{}^2 + \varepsilon_{\mathrm{L}}^2}},\end{aligned} \tag{77}$$

where $\bar{\zeta}_{\mathrm{L}} \triangleq \|J_{\mathrm{L}}\|^2$ is *unknown*, and $\Xi_{\mathrm{L}} \triangleq \|\Psi_{\mathrm{L}}\|\Big(\|\Psi_{\mathrm{L}}\dot{\alpha}_{\Theta\mathrm{L}} + \dot{\Psi}_{\mathrm{L}}\alpha_{\Theta\mathrm{L}}\| + \|\mathbb{S}(\Psi_{\mathrm{L}}\dot{\Theta}_{\mathrm{L}})\|\|\Psi_{\mathrm{L}}\alpha_{\Theta\mathrm{L}}\|\Big)$ is known.

### C. Step 5 of Backstepping Design

From (21) and (27), we have

$$\underbrace{\begin{bmatrix} I_3 & I_3 & \cdots & I_3\\ \mathbb{S}(r_1) & \mathbb{S}(r_2) & \cdots & \mathbb{S}(r_N)\end{bmatrix}}_{P}\begin{bmatrix} T_{\mathrm{d}1}e_{\mathrm{d}1}\\ \vdots\\ T_{\mathrm{d}N}e_{\mathrm{d}N}\end{bmatrix} = \begin{bmatrix} R_{\mathrm{dL}}^{\mathrm{T}}F_{\mathrm{dL}}\\ M_{\mathrm{dL}}\end{bmatrix}, \tag{78}$$

where $P$ has full row rank under Assumption 4.

### D. Step 6 of Backstepping Design

The derivative of $V_1$ with respect to time leads to

$$\begin{aligned}\dot{V}_1 &= \sum_{i=1}^{N}\Big(\dot{V}_{\mathrm{e}i} + \sum_{j=1, j\neq i}^{N}\dot{V}_{\mathrm{e}ij}\Big)\\ &= \sum_{i=1}^{N}\Big(\eta_{\mathrm{e}i}\dot{\eta}_{\mathrm{e}i} + \sum_{j=1, j\neq i}^{N}\eta_{\mathrm{e}ij}\dot{\eta}_{\mathrm{e}ij}\Big).\end{aligned} \tag{79}$$

First we examine the dynamics for $\eta_{\mathrm{e}i}$ $(i = 1, \cdots, N)$. From (15), we have

$$\begin{aligned}\dot{\eta}_{\mathrm{e}i} &= \frac{\partial\eta_{\mathrm{e}i}}{\partial\Omega_{d\mathrm{H}i}}\dot{\Omega}_{d\mathrm{H}i} + \frac{\partial\eta_{\mathrm{e}i}}{\partial d_{\mathrm{e}i}}\dot{d}_{\mathrm{e}i}\\ &= \frac{\partial\eta_{\mathrm{e}i}}{\partial d_{\mathrm{e}i}}\frac{1}{d_{\mathrm{e}i}}(x_i - x_{\mathrm{d}i})\dot{x}_i + \frac{\partial\eta_{\mathrm{e}i}}{\partial d_{\mathrm{e}i}}\frac{1}{d_{\mathrm{e}i}}(y_i - y_{\mathrm{d}i})\dot{y}_i\\ &\quad + \frac{\partial\eta_{\mathrm{e}i}}{\partial d_{\mathrm{e}i}}\frac{1}{d_{\mathrm{e}i}}(z_i - z_{\mathrm{d}i})\dot{z}_i - \xi_i,\end{aligned} \tag{80}$$

where

$$\begin{aligned}\xi_i &\triangleq \frac{\partial\eta_{\mathrm{e}i}}{\partial d_{\mathrm{e}i}}\frac{1}{d_{\mathrm{e}i}}(x_i - x_{\mathrm{d}i})\dot{x}_{\mathrm{d}i} + \frac{\partial\eta_{\mathrm{e}i}}{\partial d_{\mathrm{e}i}}\frac{1}{d_{\mathrm{e}i}}(y_i - y_{\mathrm{d}i})\dot{y}_{\mathrm{d}i}\\ &\quad + \frac{\partial\eta_{\mathrm{e}i}}{\partial d_{\mathrm{e}i}}\frac{1}{d_{\mathrm{e}i}}(z_i - z_{\mathrm{d}i})\dot{z}_{\mathrm{d}i} - \frac{\partial\eta_{\mathrm{e}i}}{\partial\Omega_{d\mathrm{H}i}}\dot{\Omega}_{d\mathrm{H}i}.\end{aligned}$$

Hence for $\dot{V}_{\mathrm{e}i}$ $(i = 1, \cdots, N)$ we have

$$\begin{aligned}\dot{V}_{\mathrm{e}i} &= \eta_{\mathrm{e}i}\frac{\partial\eta_{\mathrm{e}i}}{\partial d_{\mathrm{e}i}}\frac{1}{d_{\mathrm{e}i}}(x_i - x_{\mathrm{d}i})\dot{x}_i + \eta_{\mathrm{e}i}\frac{\partial\eta_{\mathrm{e}i}}{\partial d_{\mathrm{e}i}}\frac{1}{d_{\mathrm{e}i}}(y_i - y_{\mathrm{d}i})\dot{y}_i\\ &\quad + \eta_{\mathrm{e}i}\frac{\partial\eta_{\mathrm{e}i}}{\partial d_{\mathrm{e}i}}\frac{1}{d_{\mathrm{e}i}}(z_i - z_{\mathrm{d}i})\dot{z}_i - \eta_{\mathrm{e}i}\xi_i.\end{aligned} \tag{81}$$

Similarly, for $\dot{V}_{\mathrm{e}ij}$ $(i, j = 1, \cdots, N,\ j \neq i)$ we have

$$\begin{aligned}&\dot{V}_{\mathrm{e}ij}\\ &= \eta_{\mathrm{e}ij}\frac{\partial\eta_{\mathrm{e}ij}}{\partial d_{\mathrm{e}ij}}\frac{1}{d_{ij}}(x_i - x_j)\dot{x}_i + \eta_{\mathrm{e}ij}\frac{\partial\eta_{\mathrm{e}ij}}{\partial d_{\mathrm{e}ij}}\frac{1}{d_{ij}}(y_i - y_j)\dot{y}_i\\ &\quad + \eta_{\mathrm{e}ij}\frac{\partial\eta_{\mathrm{e}ij}}{\partial d_{\mathrm{e}ij}}\frac{1}{d_{ij}}(z_i - z_j)\dot{z}_i - \eta_{\mathrm{e}ij}\frac{\partial\eta_{\mathrm{e}ij}}{\partial d_{\mathrm{e}ij}}\frac{1}{d_{ij}}(x_i - x_j)\dot{x}_j\\ &\quad - \eta_{\mathrm{e}ij}\frac{\partial\eta_{\mathrm{e}ij}}{\partial d_{\mathrm{e}ij}}\frac{1}{d_{ij}}(y_i - y_j)\dot{y}_j - \eta_{\mathrm{e}ij}\frac{\partial\eta_{\mathrm{e}ij}}{\partial d_{\mathrm{e}ij}}\frac{1}{d_{ij}}(z_i - z_j)\dot{z}_j\\ &\quad - \eta_{\mathrm{e}ij}\xi_{\mathrm{e}ij},\end{aligned} \tag{82}$$

where

$$\begin{aligned}\xi_{\mathrm{e}ij} &\triangleq \frac{\partial\eta_{\mathrm{e}ij}}{\partial d_{\mathrm{e}ij}}\dot{\vartheta}_{ij} - \left(\frac{\partial\eta_{\mathrm{e}ij}}{\partial\Omega_{\mathrm{H}ij}}\dot{\Omega}_{\mathrm{H}ij} + \frac{\partial\eta_{\mathrm{e}ij}}{\partial\Omega_{\mathrm{W}ij}}\dot{\Omega}_{\mathrm{W}ij}\right)\\ &= \frac{\partial\eta_{\mathrm{e}ij}}{\partial d_{\mathrm{e}ij}}\frac{1}{\vartheta_{ij}}(x_{\mathrm{d}i} - x_{\mathrm{d}j})(\dot{x}_{\mathrm{d}i} - \dot{x}_{\mathrm{d}j})\\ &\quad + \frac{\partial\eta_{\mathrm{e}ij}}{\partial d_{\mathrm{e}ij}}\frac{1}{\vartheta_{ij}}(y_{\mathrm{d}i} - y_{\mathrm{d}j})(\dot{y}_{\mathrm{d}i} - \dot{y}_{\mathrm{d}j})\\ &\quad + \frac{\partial\eta_{\mathrm{e}ij}}{\partial d_{\mathrm{e}ij}}\frac{1}{\vartheta_{ij}}(z_{\mathrm{d}i} - z_{\mathrm{d}j})(\dot{z}_{\mathrm{d}i} - \dot{z}_{\mathrm{d}j})\\ &\quad - \left(\frac{\partial\eta_{\mathrm{e}ij}}{\partial\Omega_{\mathrm{H}ij}}\dot{\Omega}_{\mathrm{H}ij} + \frac{\partial\eta_{\mathrm{e}ij}}{\partial\Omega_{\mathrm{W}ij}}\dot{\Omega}_{\mathrm{W}ij}\right).\end{aligned}$$

### E. Proof of Theorem 1

*Proof:* First of all, from (47), we have

$$V_{\mathrm{UAV1}}(t) \leq \Big(V_{\mathrm{UAV1}}(0) - \frac{\varrho_1}{\kappa_1}\Big)e^{-\kappa_1 t} + \frac{\varrho_1}{\kappa_1}, \tag{83}$$

hence $V_{\mathrm{UAV1}}$ is uniformly bounded. The boundedness of $V_{\mathrm{UAV1}}$ implies boundedness of $\eta_{\mathrm{eL}}$, $\eta_{ei}$, and $\eta_{eij}$. Hence, the constraints requirements (11), (12), and (13) are satisfied during the operation.

Moreover, we have $\limsup_{t\to\infty} V_{\mathrm{UAV1}} = \frac{\varrho_1}{\kappa_1}$, hence $\frac{1}{2}\eta_{\mathrm{eL}}^2 \leq \frac{\varrho_1}{\kappa_1}$ when $t \to \infty$, therefore $\eta_{\mathrm{eL}}$ will converge to the set (48). Similar relationships hold for $\eta_{ei}$, $\eta_{eij}$, and $z_{3\mathrm{L}}$. Furthermore, boundedness of the adaptive estimates $\hat{\delta}_{1\mathrm{L}}$, $\hat{\rho}_{J\mathrm{L}}$, $\hat{\zeta}_{\mathrm{L}}$, $\hat{\delta}_{2\mathrm{L}}$, $\hat{\delta}_i$, $\hat{\rho}_{mi}$, as well as boundedness of the fictitious error $z_{2\mathrm{L}}$ and $z_{2i}$ $(i = 1, \cdots, N)$, can be implied by the boundedness of $V_{\mathrm{UAV1}}$. The boundedness of these variables implies the boundedness of the desired cable tension $T_{\mathrm{d}i}$ and the control law $u_i$ $(i = 1, \cdots, N)$.

Next, note that in the range $d_{\mathrm{eL}} < \Omega_{d\mathrm{HL}}$ and $d_{ei} < \Omega_{d\mathrm{H}i}$ $(i = 1, \cdots, N)$, (11) and (12) give rise to the range for $d_{\mathrm{eL}}$ and $d_{ei}$ given as in (50). Besides, within the range of (13), $\eta_{eij}$ is quadratically related to $d_{eij}$. Hence, satisfying the constraints (13) means that the relative distance tracking errors $d_{eij}$ will be confined in the ranges defined by (51). ■

### F. Step 8 of Backstepping Design

First, we need to extract the reference attitude from the position control design. Recall that $u_i = F_i R_{\mathrm{d}i} e_z$, and from (41) we have

$$u_i = F_i \begin{bmatrix} \mathrm{c}\phi_{\mathrm{d}i}\mathrm{s}\theta_{\mathrm{d}i}\mathrm{c}\psi_{\mathrm{d}i} + \mathrm{s}\phi_{\mathrm{d}i}\mathrm{s}\psi_{\mathrm{d}i} \\ \mathrm{c}\phi_{\mathrm{d}i}\mathrm{s}\theta_{\mathrm{d}i}\mathrm{s}\psi_{\mathrm{d}i} - \mathrm{s}\phi_{\mathrm{d}i}\mathrm{c}\psi_{\mathrm{d}i} \\ \mathrm{c}\phi_{\mathrm{d}i}\mathrm{c}\theta_{\mathrm{d}i} \end{bmatrix}, \tag{84}$$

in which we recall that $F_i$ is the thrust of the $i$th quadrotor. Here, for any designated reference yaw angle $\psi_{\mathrm{d}i}$ satisfying Assumption 1, we define

$$F_i = \|u_i\|, \tag{85}$$

$$\phi_{\mathrm{d}i} = \arcsin\Big(\frac{u_{i1}\mathrm{s}\psi_{\mathrm{d}i} - u_{i2}\mathrm{c}\psi_{\mathrm{d}i}}{\|u_i\|}\Big), \tag{86}$$

$$\theta_{\mathrm{d}i} = \arctan\Big(\frac{u_{i1}\mathrm{c}\psi_{\mathrm{d}i} + u_{i2}\mathrm{s}\psi_{\mathrm{d}i}}{u_{i3}}\Big), \tag{87}$$

where $u_i = [u_{i1},\ u_{i2},\ u_{i3}]^{\mathrm{T}} \in \mathbb{R}^3$.

Next, taking derivative of $\phi_{\mathrm{d}i}$ in (86) and $\theta_{\mathrm{d}i}$ in (87) with respect to time yields

$$\dot{\phi}_{\mathrm{d}i} = \frac{\partial\phi_{\mathrm{d}i}}{\partial u_{i1}}\dot{u}_{i1} + \frac{\partial\phi_{\mathrm{d}i}}{\partial u_{i2}}\dot{u}_{i2} + \frac{\partial\phi_{\mathrm{d}i}}{\partial u_{i3}}\dot{u}_{i3} + \frac{\partial\phi_{\mathrm{d}i}}{\partial\psi_{\mathrm{d}i}}\dot{\psi}_{\mathrm{d}i},$$

$$\dot{\theta}_{\mathrm{d}i} = \frac{\partial\theta_{\mathrm{d}i}}{\partial u_{i1}}\dot{u}_{i1} + \frac{\partial\theta_{\mathrm{d}i}}{\partial u_{i2}}\dot{u}_{i2} + \frac{\partial\theta_{\mathrm{d}i}}{\partial u_{i3}}\dot{u}_{i3} + \frac{\partial\theta_{\mathrm{d}i}}{\partial\psi_{\mathrm{d}i}}\dot{\psi}_{\mathrm{d}i},$$

where $u_{i1}$, $u_{i2}$, $u_{i3}$ are bounded according to Theorem 1, and $\psi_{\mathrm{d}i}$ and $\dot{\psi}_{\mathrm{d}i}$ are bounded according to Assumption 1, such that the terms $\frac{\partial\phi_{\mathrm{d}i}}{\partial u_{i1}}$, $\frac{\partial\phi_{\mathrm{d}i}}{\partial u_{i2}}$, $\frac{\partial\phi_{\mathrm{d}i}}{\partial u_{i3}}$, $\frac{\partial\phi_{\mathrm{d}i}}{\partial\psi_{\mathrm{d}i}}$, $\frac{\partial\theta_{\mathrm{d}i}}{\partial u_{i1}}$, $\frac{\partial\theta_{\mathrm{d}i}}{\partial u_{i2}}$, $\frac{\partial\theta_{\mathrm{d}i}}{\partial u_{i3}}$, and $\frac{\partial\theta_{\mathrm{d}i}}{\partial\psi_{\mathrm{d}i}}$ are all bounded. The result of differentiating $u_i$ in (41) with respect to time can be combined with Theorem 1 to conclude the boundedness of $\dot{u}_{i1}$, $\dot{u}_{i2}$, and $\dot{u}_{i3}$. Therefore, $\dot{\Theta}_{\mathrm{d}i}$ is bounded, which satisfies $\|\dot{\Theta}_{\mathrm{d}i}\| \leq \bar{\Theta}_{\mathrm{d}i}$, where $\bar{\Theta}_{\mathrm{d}i}$ is an *unknown* positive constant. Note that for any $\nu_i > 0$,

$$z_{3i}^{\mathrm{T}}\dot{\Theta}_{\mathrm{d}i} \leq \|z_{3i}\|\bar{\Theta}_{\mathrm{d}i} \leq \frac{1}{2\nu_i}\bar{\Theta}_{\mathrm{d}i}^2 + \frac{\nu_i}{2}z_{3i}^{\mathrm{T}}z_{3i}.$$

Therefore, we can obtain the result shown in (57).

### G. Step 9 of Backstepping Design

The rate of change of $V_4$ is

$$\dot{V}_4 = \sum_{i=1}^{N} z_{4i}^{\mathrm{T}}\Big(\Psi_i^{\mathrm{T}}J_i^{\mathrm{T}}\tau_i - M_i\dot{\alpha}_{\Theta i} - C_i\alpha_{\Theta i}\Big), \tag{88}$$

where, for $z_{4i}^{\mathrm{T}}(-M_i\dot{\alpha}_{\Theta i} - C_i\alpha_{\Theta i})$, we can get

$$\begin{aligned} & z_{4i}^{\mathrm{T}}(-M_i\dot{\alpha}_{\Theta i} - C_i\alpha_{\Theta i}) \\ &= -z_{4i}^{\mathrm{T}}\Psi_i^{\mathrm{T}}J_i^{\mathrm{T}}J_i\Big(\Psi_i(K_{3i} + \frac{\nu_i}{2})(\dot{\Theta}_i - \dot{\Theta}_{\mathrm{d}i}) + \dot{\Psi}_i\alpha_{\Theta i}\Big) \\ &\quad - z_{4i}^{\mathrm{T}}\Psi_i^{\mathrm{T}}J_i^{\mathrm{T}}\mathbb{S}(\Psi_i\dot{\Theta}_i)J_i\Psi_i\alpha_{\Theta i} \\ &\leq \|z_{4i}\|\|\Psi_i\|\|J_i\|^2\Big(\|\dot{\Psi}_i\alpha_{\Theta i}\| + \|(K_{3i} + \frac{\nu_i}{2})\Psi_i\dot{\Theta}_i\| \\ &\quad + \|\mathbb{S}(\Psi_i\dot{\Theta}_i)\|\|\Psi_i\alpha_{\Theta i}\| + \bar{\Theta}_{\mathrm{d}i}\|(K_{3i} + \frac{\nu_i}{2})\Psi_i\|\Big) \\ &< \varepsilon_i\bar{\zeta}_i + \bar{\zeta}_i\frac{\|z_{4i}\|^2\,\Xi_i{}^2}{\sqrt{\|z_{4i}\|^2\,\Xi_i{}^2 + \varepsilon_i^2}}, \end{aligned} \tag{89}$$

where $\bar{\zeta}_i \triangleq \|J_i\|^2(1 + \bar{\Theta}_{\mathrm{d}i})$ is *unknown*, and $\Xi_i \triangleq \|\Psi_i\|\Big(\|\dot{\Psi}_i\alpha_{\Theta i}\| + \|(K_{3i} + \frac{\nu_i}{2})\Psi_i\dot{\Theta}_i\| + \|\mathbb{S}(\Psi_i\dot{\Theta}_i)\|\|\Psi_i\alpha_{\Theta i}\| + \|(K_{3i} + \frac{\nu_i}{2})\Psi_i\|\Big)$ is known.

### H. Proof of Theorem 2

*Proof:* First of all, (64) leads to

$$V_{\mathrm{UAV2}}(t) \leq \Big(V_{\mathrm{UAV2}}(0) - \frac{\varrho_2}{\kappa_2}\Big)e^{-\kappa_2 t} + \frac{\varrho_2}{\kappa_2}, \tag{90}$$

hence $V_{\mathrm{UAV2}}$ is uniformly bounded.

Next, we have $\limsup_{t\to\infty} V_{\mathrm{UAV2}} = \frac{\varrho_2}{\kappa_2}$, hence $\frac{1}{2}z_{3i}^2 \leq \frac{\varrho_2}{\kappa_2}$ when $t \to \infty$, therefore $z_{3i}$ will converge to the set (65). Furthermore, boundedness of the adaptive estimates $\hat{\rho}_{Ji}$ and $\hat{\zeta}_i$, as well as boundedness of the fictitious error $z_{4i}$ $(i = 1, \cdots, N)$, are now apparent since $V_{\mathrm{UAV2}}$ is bounded. Therefore, it is straightforward to prove the boundedness of the torque laws (58) and (59), as well as adaptive laws (60) and (61). ■

## ACKNOWLEDGMENT

The authors appreciate an Editor, an Associate Editor, and Reviewers from the IEEE TRANSACTIONS ON INTELLIGENT TRANSPORTATION SYSTEMS for the helpful comments and constructive suggestions during the review process.

## REFERENCES


[1] D. K. D. Villa, A. S. Brandao, and M. Sarcinelli-Filho, "Load transportation using quadrotors: A survey of experimental results," in *Proc. Int. Conf. Unmanned Aircr. Syst. (ICUAS)*, Jun. 2018, pp. 84–93.

[2] D. K. Villa, A. S. Brandão, and M. Sarcinelli-Filho, "A survey on load transportation using multirotor UAVs," *J. Intell. Robot. Syst.*, vol. 98, pp. 267–296, May 2020.

[3] G. Skorobogatov, C. Barrado, and E. Salamí, "Multiple UAV systems: A survey," *Unmanned Syst.*, vol. 8, no. 2, pp. 149–169, Apr. 2020.

[4] T. Elmokadem and A. V. Savkin, "Towards fully autonomous UAVs: A survey," *Sensors*, vol. 21, no. 18, p. 6223, Sep. 2021.

[5] N. S. Zuniga, F. Munoz, M. A. Marquez, E. S. Espinoza, and L. R. G. Carrillo, "Load transportation using single and multiple quadrotor aerial vehicles with swing load attenuation," in *Proc. Int. Conf. Unmanned Aircr. Syst. (ICUAS)*, Jun. 2018, pp. 269–278.

[6] D. K. D. Villa, A. S. Brandao, and M. Sarcinelli-Filho, "Rod-shaped payload transportation using multiple quadrotors," in *Proc. Int. Conf. Unmanned Aircr. Syst. (ICUAS)*, Jun. 2019, pp. 1036–1040.

[7] K. Klausen, T. I. Fossen, T. A. Johansen, and A. P. Aguiar, "Cooperative path-following for multirotor UAVs with a suspended payload," in *Proc. IEEE Conf. Control Appl. (CCA)*, Sep. 2015, pp. 1354–1360.

[8] I. H. B. Pizetta, A. S. Brandao, and M. Sarcinelli-Filho, "Cooperative load transportation using three quadrotors," in *Proc. Int. Conf. Unmanned Aircr. Syst. (ICUAS)*, Jun. 2019, pp. 644–650.

[9] B. E. Jackson, T. A. Howell, K. Shah, M. Schwager, and Z. Manchester, "Scalable cooperative transport of cable-suspended loads with UAVs using distributed trajectory optimization," *IEEE Robot. Autom. Lett.*, vol. 5, no. 2, pp. 3368–3374, Apr. 2020.

[10] L. Saiella, A. Cristofaro, M. Ferro, and M. Vendittelli, "Fault-tolerant formation control of a team of quadrotors with a suspended payload," in *Proc. Int. Conf. Unmanned Aircr. Syst. (ICUAS)*, Jun. 2021, pp. 1–9.

[11] K. Klausen, C. Meissen, T. I. Fossen, M. Arcak, and T. A. Johansen, "Cooperative control for multirotors transporting an unknown suspended load under environmental disturbances," *IEEE Trans. Control Syst. Technol.*, vol. 28, no. 2, pp. 653–660, Mar. 2018.

[12] S. Thapa, H. Bai, and J. Á. Acosta, "Cooperative aerial load transport with force control," *IFAC-PapersOnLine*, vol. 51, no. 12, pp. 38–43, 2018.

[13] B. Shirani, M. Najafi, and I. Izadi, "Cooperative load transportation using multiple UAVs," *Aerosp. Sci. Technol.*, vol. 84, pp. 158–169, Jan. 2019.

[14] X. Zhang et al., "Self-triggered based coordinate control with low communication for tethered multi-UAV collaborative transportation," *IEEE Robot. Autom. Lett.*, vol. 6, no. 2, pp. 1559–1566, Apr. 2021.

[15] G. Wu and K. Sreenath, "Geometric control of multiple quadrotors transporting a rigid-body load," in *Proc. 53rd IEEE Conf. Decis. Control*, Dec. 2014, pp. 6141–6148.

[16] T. Lee, "Geometric control of quadrotor UAVs transporting a cable-suspended rigid body," *IEEE Trans. Control Syst. Technol.*, vol. 26, no. 1, pp. 255–264, Jan. 2017.

[17] T. Bacelar, J. Madeiras, R. Melicio, C. Cardeira, and P. Oliveira, "On-board implementation and experimental validation of collaborative transportation of loads with multiple UAVs," *Aerosp. Sci. Technol.*, vol. 107, Dec. 2020, Art. no. 106284.

[18] G. A. Cardona, M. Arevalo-Castiblanco, D. Tellez-Castro, J. Calderon, and E. Mojica-Nava, "Robust adaptive synchronization of interconnected heterogeneous quadrotors transporting a cable-suspended load," in *Proc. IEEE Int. Conf. Robot. Autom. (ICRA)*, May 2021, pp. 31–37.

[19] H. Lee, H. Kim, and H. J. Kim, "Planning and control for collision-free cooperative aerial transportation," *IEEE Trans. Autom. Sci. Eng.*, vol. 15, no. 1, pp. 189–201, Jan. 2016.

[20] I. H. B. Pizetta, A. S. Brandão, and M. Sarcinelli-Filho, "Avoiding obstacles in cooperative load transportation," *ISA Trans.*, vol. 91, pp. 253–261, Aug. 2019.

[21] K. Kotani, Z. Guo, T. Namerikawa, and Z. Qu, "Cooperative transport control by a multicopter system," *IET Control Theory Appl.*, vol. 15, no. 6, pp. 861–876, Apr. 2021.

[22] A. Hegde and D. Ghose, "Multi-UAV collaborative transportation of payloads with obstacle avoidance," *IEEE Control Syst. Lett.*, vol. 6, pp. 926–931, 2021.

[23] J. Geng and J. W. Langelaan, "Implementation and demonstration of coordinated transport of a slung load by a team of rotorcraft," in *Proc. AIAA Scitech Forum*, 2019, p. 913.

[24] J. Geng and J. W. Langelaan, "Cooperative transport of a slung load using load-leading control," *J. Guid., Control, Dyn.*, vol. 43, no. 7, pp. 1313–1331, 2020.

[25] N. Michael, J. Fink, and V. Kumar, "Cooperative manipulation and transportation with aerial robots," *Auto. Robot.*, vol. 30, no. 1, pp. 73–86, 2011.

[26] X. Jin, "Adaptive fixed-time control for MIMO nonlinear systems with asymmetric output constraints using universal barrier functions," *IEEE Trans. Autom. Control*, vol. 64, no. 7, pp. 3046–3053, Jul. 2019.

[27] X. Jin, J. Liang, S.-L. Dai, and D. Guo, "Adaptive Line-of-Sight tracking control for a tractor-trailer vehicle system with multiple constraints," *IEEE Trans. Intell. Transp. Syst.*, vol. 23, no. 8, pp. 11349–11360, Aug. 2021.

[28] X. Jin, S.-L. Dai, and J. Liang, "Adaptive constrained formation tracking control for a tractor-trailer mobile robot team with multiple constraints," *IEEE Trans. Autom. Control*, early access, Feb. 15, 2022, doi: 10.1109/TAC.2022.3151846.

[29] C. Wen, J. Zhou, Z. Liu, and H. Su, "Robust adaptive control of uncertain nonlinear systems in the presence of input saturation and external disturbance," *IEEE Trans. Autom. Control*, vol. 56, no. 7, pp. 1672–1678, Jul. 2011.

[30] S. Mastellone, D. M. Stipanović, C. R. Graunke, K. A. Intlekofer, and M. W. Spong, "Formation control and collision avoidance for multi-agent non-holonomic systems: Theory and experiments," *Int. J. Robot. Res.*, vol. 27, no. 1, pp. 107–126, Jan. 2008.

[31] M. Chen, G. Tao, and B. Jiang, "Dynamic surface control using neural networks for a class of uncertain nonlinear systems with input saturation," *IEEE Trans. Neural Netw. Learn. Syst.*, vol. 26, no. 9, pp. 2086–2097, Sep. 2015.


**Xu Jin** (Member, IEEE) received the Bachelor of Engineering (B.Eng.) degree (Hons.) in electrical and computer engineering from the National University of Singapore, Singapore, the Master of Applied Science (M.A.Sc.) degree in electrical and computer engineering from the University of Toronto, Toronto, ON, Canada, and the Master of Science (M.S.) degree in mathematics and the Doctor of Philosophy (Ph.D.) degree in aerospace engineering from the Georgia Institute of Technology, Atlanta, GA, USA.

He is currently an Assistant Professor with the Department of Mechanical and Aerospace Engineering, University of Kentucky, Lexington, KY, USA. His current research interests include adaptive and iterative learning control with applications to intelligent vehicles, autonomous robots, and nonlinear multiagent systems.

**Zhongjun Hu** received the B.Eng. degree in automation from the College of Information Engineering, Zhejiang University of Technology, Hangzhou, China, in 2018, and the M.S. degree in electrical and computer engineering from The Ohio State University, Columbus, OH, USA, in 2020. He is currently pursuing the Ph.D. degree with the Department of Mechanical and Aerospace Engineering, University of Kentucky, Lexington, KY, USA.

His research interests include adaptive control and its application of multiagent systems.